REDUCTION OF SHAFT VOLTAGES AND BEARING CURRENTS IN FIVE-PHASE INDUCTION MOTORS

A Thesis

by

HUSSAIN A. I. A. HUSSAIN

Submitted to the Office of Graduate Studies of
Texas A&M University
in partial fulfillment of the requirements for the degree of

MASTER OF SCIENCE

May 2012

Major Subject: Electrical Engineering

Reduction of Shaft Voltages and Bearing Currents in Five-Phase Induction Motors

REDUCTION OF SHAFT VOLTAGES AND BEARING CURRENTS IN FIVE-PHASE INDUCTION MOTORS

A Thesis

by

HUSSAIN A. I. A. HUSSAIN

Submitted to the Office of Graduate Studies of
Texas A&M University
in partial fulfillment of the requirements for the degree of

MASTER OF SCIENCE

Approved by:

Chair of Committee,	Hamid A. Toliyat
Committee Members,	Robert Balog
	Shankar P. Bhattacharyya
	Won-jong Kim
Head of Department,	Costas N. Georghiades

May 2012

Major Subject: Electrical Engineering

ABSTRACT

Reduction of Shaft Voltages and Bearing Currents in Five-Phase Induction Motor.

(May 2012)

Hussain A. I. A. Hussain, B.Sc Electrical Engineering, Kuwait University

Chair of Advisory Committee: Dr. Hamid A. Toliyat

Induction motors are commonly used in numerous industrial applications. To maintain a reliable operation of the motor, it is important to identify the potential faults that may cause the motor to fail. Bearing failures are one of the main causes of motor breakdown. The causes of bearing damage have been studied in detail for a long time. In some cases, bearing failed due to the current passing through them. In this thesis, bearing currents in an inverter driven five-phase induction motor are studied and a new solution is proposed.

First, theory of shaft voltage and bearing current are presented. The causes are identified and current solutions are discussed. Then, new switching patterns are proposed for the five-phase induction motor. The new schemes apply a modified algorithm for the space vector pulse-width-modulation (SVPWM). The system is simulated and the results of the new switching patterns are compared with the conventional switching pattern. Finally, the new schemes are experimentally tested using a digital signal processor (DSP) to drive the five-phase IGBT inverter. The experimental results verified that the

new switching pattern could reduce shaft voltages and bearing current without affecting the performance.

To my family

ACKNOWLEDGEMENTS

I would like to thank Dr. Hamid Toliyat for his continuous help and guidance throughout the course of the research.

Thanks also go to the members of my graduate study committee for their support. Also I would also like to thank my colleagues in the Advanced Electric Machines and Power Electronics (EMPE) Laboratory for their valuable help.

TABLE OF CONTENTS

Page

LIST OF FIGURES

Page

LIST OF TABLES

Page

CHAPTER I

INTRODUCTION AND LITERATURE REVIEW

1. Introduction

For the past century, induction motor was widely used in the industry due to its simple and robust construction. Since the electric power sources are available as three-phase sources, induction motors were built as three-phase machines. This was true until Pulse Width Modulated (PWM) drives were introduced which allowed the use of higher number phases. In conventional PWM drives, the three-phase voltage ac source is rectified to a dc bus. Then, an inverter is used to convert the dc bus to a controllable three-phase ac source.

It is not necessary to invert the DC bus to three phases only; it could be inverted to a different number of phases (e.g., five phases). This introduced the multiphase motors which have been studied for a long time.

In any motor, there are two bearings which support the rotating shaft with respect to the stationary frame. Usually, bearings are considered as the first point of failure in a motor. Fig. 1 shows the most common causes of bearing failure and the percentage of its occurrence. It shows that 9% of bearing failure is due to bearing currents.

In this thesis, the bearing currents in five-phase induction motors are studied. The causes and solutions are reviewed. Then, a new solution is proposed and verified experimentally.

This thesis follows the style of *IEEE Transactions on Industry Applications*.

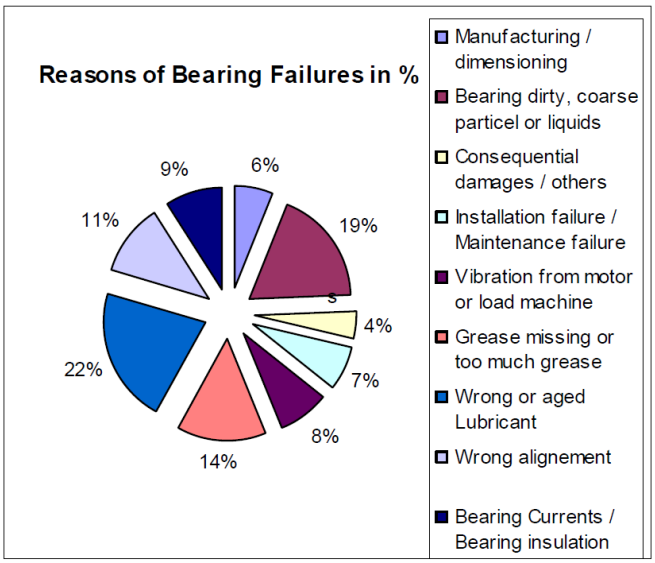

Fig. 1 : Reasons of bearing damage [1]

2. Shaft voltage generation

The theory behind shaft voltages and bearing currents is well understood today [2] - [8]. In this section, the theory is reviewed and the system is modeled. This model will be used later to simulate the system under different conditions.

In electrical machines, current flows in the windings to generate the magnetic flux and rotate the shaft. Ideally, no current flows in the shaft or other mechanical components. If an electrical current flow in the mechanical system for any reason, it may cause problems. For instance, electrical currents can reduce bearing life time and damage the bearing.

The problem of shaft voltages and bearing currents was discovered back in 1920's [9], but solved by improving motor symmetry and manufacturing tolerances. Recently, the problem was reported again when pulse width modulated (PWM) drives

were installed. Some common symptoms that indicate the existence of bearing current include: blackening the oil, scoring the shaft, noise, and pitting and fluting the bearing as shown in Fig. 2:

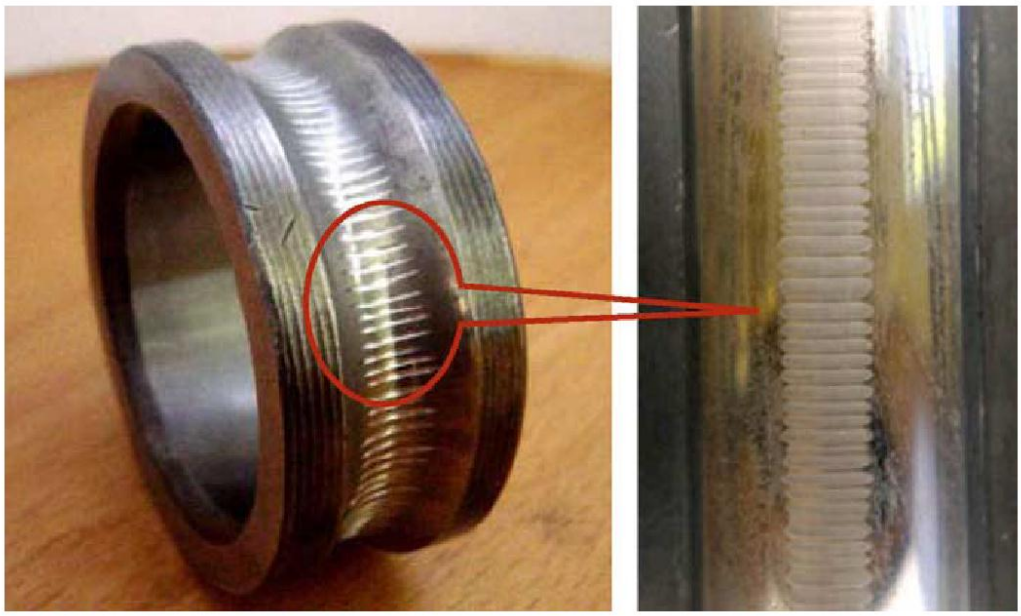

Fig. 2 : Fluting the bearing [10]

Fig. 3 shows a model of the stator of a three-phase induction motor connected to a voltage source.

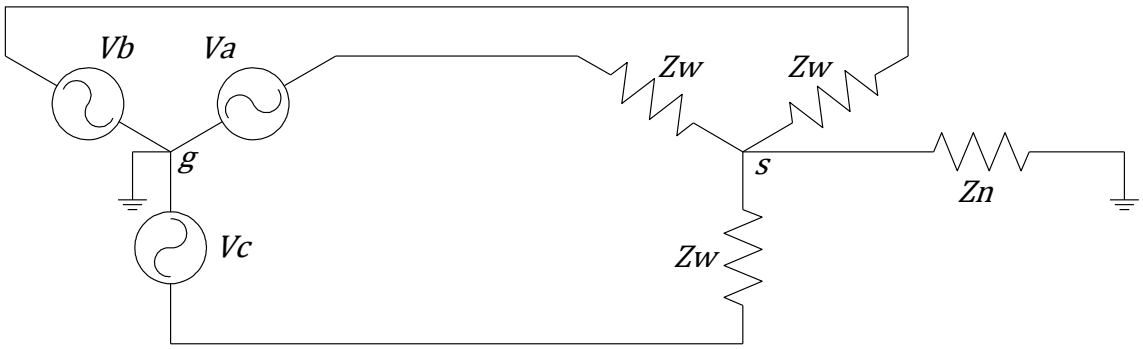

Fig. 3 : Motor stator model

In motor design, the stator neutral node (s) is not connected directly to ground. Thus, it is usually assumed as an ideal open circuit. Practically speaking, there will always be an impedance that exists between the neutral node and the ground which is represented as Zn in Fig. 3. Current will flow in Zn impedance only if there is a voltage between node (s) and the ground.

If the three-phase voltage source was a balance sinusoidal source, no voltage will appear on node (s) as shown in Fig. 4(b). On the other hand, when the voltage source is of a PWM type, a high frequency voltage exists as shown in Fig. 5(d). The theory behind this phenomenon could be explained by the zero sequence circuit presented in chapter V. Therefore, the problem will exist in PWM drives but not in sinusoidal voltage sources.

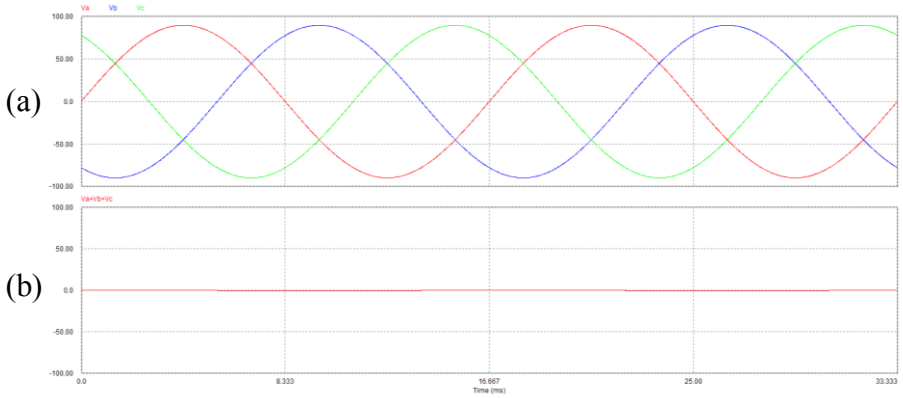

Fig. 4 : (a) Sinusoidal three-phase volatge source (b) neutral point voltage

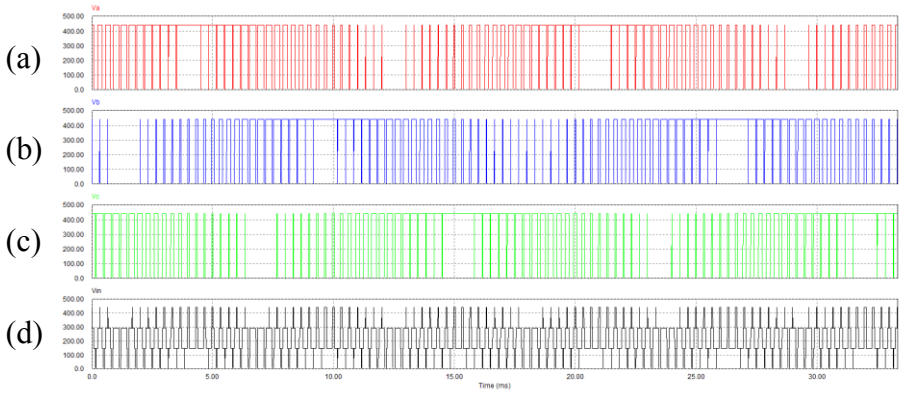

Fig. 5 : PWM volatge source (a) Va (b) Vb (c) Vc (d) neutral point voltage

3. Parasitic capacitances inside motors

Capacitive discharge current is caused by the parasitic capacitive coupling. It is more likely to occur in small motors whereas large motors will suffer from circulating currents [11]. The paths that the current could flow through are presented in Fig. 6.

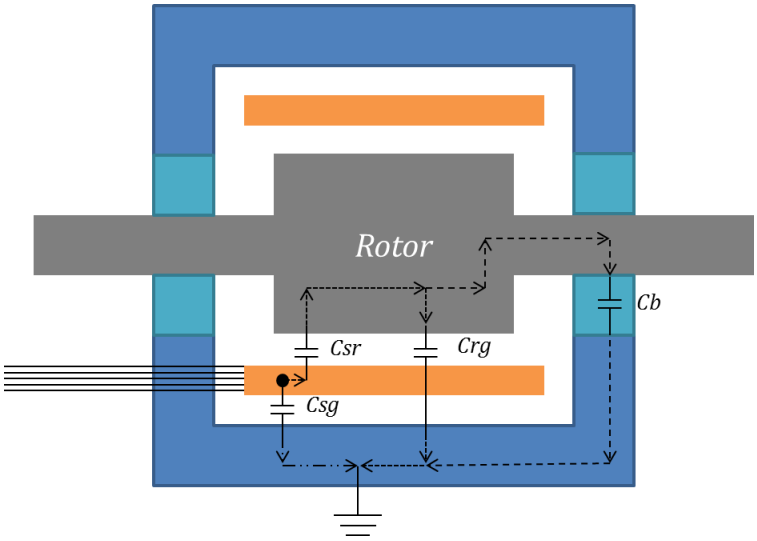

Fig. 6 : Current paths in the mechanical system

These current could be represented as follows:

1) From stator's neutral to ground,
2) From stator's neutral to shaft to ground,
3) From stator's neutral to shaft to bearing to ground.

Thus, the system could be modeled as shown in Fig. 7 [2]:

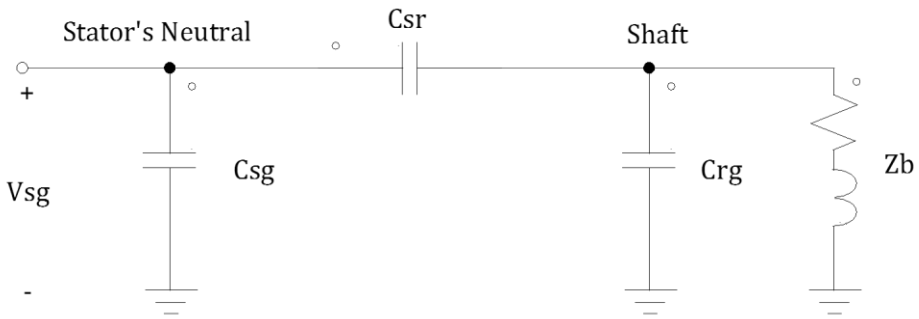

Fig. 7 : Model of parasitic capacitance in the motor

Where,

- Csg is the capacitance between stator's neutral and ground,
- Csr is the capacitance between stator's neutral and shaft,
- Crg is the capacitance between shaft and ground,
- Zb is the impedance of the bearing.

4. Bearing impedance model

Fig. 8 (a) shows the electrical model of each ball of the bearing. The model includes the resistances of the outer race, inner race and the ball. It also considers the capacitance of the balls and the gap. Moreover, the model represents the discharge mechanism as nonlinear impedance. The model could be reduced to the equivalent model shown in Fig. 8 (b) [2].

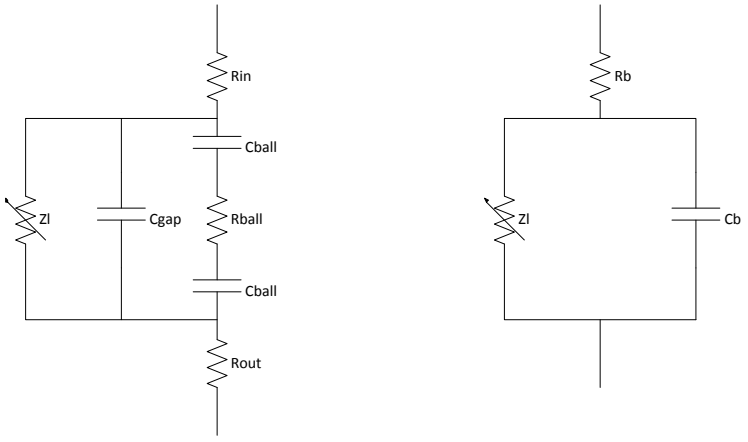

(a) (b)

Fig. 8 : (a) Per ball model, (b) Model of bearings

The nonlinear bearing impedance could be modeled as a DIAC that will switch to a very low impedance path if the voltage exceeds the breakdown voltage. The break down voltage depends on the asperity contact area and the lubricant film thickness between the balls and bearing races [3]. The final bearing model is shown in Fig. 9.

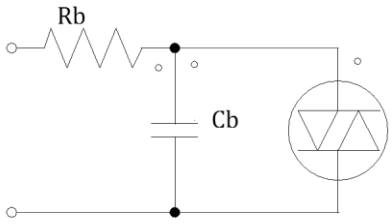

Fig. 9 : Final bearing model

From this bearing model, it could be inferred that two types of current may flow through the bearing:

1) dv/dt current: If the shaft voltage did not exceed the break down voltage, the current could be expressed as:

$$I_b = C\frac{dV_{shaft}}{dt} \qquad (1)$$

2) Electric Discharge Machining (EDM) current: If the voltage exceeds the breakdown, the bearing is shorted and a high magnitude current pulse flow through the bearing.

5. Solutions to the problem

Presently, many solutions are suggested to this problem. These include:

A. Bearing insulation

Insulating the bearings will increase the resistance of the bearing and reduces the current flow. It may be implemented in two ways: insulating both bearing's pedestals or by using hybrid bearing (Ceramic balls). It should be noted, however, that this will only transfer the problem to the coupling and load. Therefore, the coupling should be insulated too.

B. Shaft grounding

Grounding the shaft will provide an alternative path for the current to flow in. It is applied in three methods:

1) Grounding brush,
2) Grommet,
3) Ring.

C. Conductive grease

Conductive grease will short the current and no high discharge current will flow. The main problem with this method is that conductive particles in these lubricants increase mechanical wear to the bearing.

D. dv/dt filter

Common mode reactor could be used in series with the motor in two ways:

1. Active cancellation,
2. Low-pass filtering.

E. Faraday shield

A grounded conductive material installed between rotor and stator creates a Faraday shield. It reduces capacitive coupled currents across the air gap and minimizes shaft voltage [4].

F. Shielded three-phase cable

A shielded cable can improve the high frequency grounding by providing a low impedance path between the drive and the motor.

G. New inverter topology

Using a five-phase control method to reduce neutral's stator voltage and thus EDM bearing currents. One crucial and successful way, is to modify the switching scheme. This will be the topic presented in the following chapters.

CHAPTER II

QD0 TRANSFORMATION

1. Introduction

The qd0 transformation is commonly used to simplify the analysis of machine models. Basically, it transforms the three phases to two-phase system. In multiphase machines, the transformation will lead to multiple two-phase systems.

2. qd0 in three phase machine

Fig. 10 shows the abc vectors along with the qd vectors.

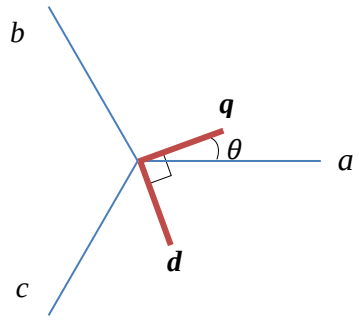

Fig. 10 : abc and qd vectors

To transform from abc frame to the qd0 frame with an arbitrary angel θ the following transformation could be used:

$$\begin{bmatrix} f_q \\ f_d \\ f_0 \end{bmatrix} = \frac{2}{3}\begin{bmatrix} \cos(\theta) & \cos\left(\theta - \frac{2\pi}{3}\right) & \cos\left(\theta + \frac{2\pi}{3}\right) \\ \sin(\theta) & \sin\left(\theta - \frac{2\pi}{3}\right) & \sin\left(\theta + \frac{2\pi}{3}\right) \\ \frac{1}{2} & \frac{1}{2} & \frac{1}{2} \end{bmatrix}\begin{bmatrix} f_a \\ f_b \\ f_c \end{bmatrix} \quad (2)$$

Or simply,

$$f^{qd0} = T(\theta)\, f^{abc} \quad (3)$$

Where T(θ) is the transformation matrix and f could represents the voltage, current or flux linkage of either the stator or the rotor. Taking the inverse,

$$\begin{bmatrix} f_a \\ f_b \\ f_c \end{bmatrix} = \begin{bmatrix} \cos(\theta) & \sin(\theta) & 1 \\ \cos\left(\theta - \frac{2\pi}{3}\right) & \sin\left(\theta - \frac{2\pi}{3}\right) & 1 \\ \cos\left(\theta + \frac{2\pi}{3}\right) & \sin\left(\theta + \frac{2\pi}{3}\right) & 1 \end{bmatrix}\begin{bmatrix} f_q \\ f_d \\ f_0 \end{bmatrix} \quad (4)$$

$$f^{abc} = T^{-1}(\theta) f^{qd0} \quad (5)$$

For a stationary qd0 reference frame, the (q) vector is assumed to be fixed and aligned with (a) vector. In the stator, the abc vectors are stationary. So θ is constant and equals zeros as shown in Fig. 11:

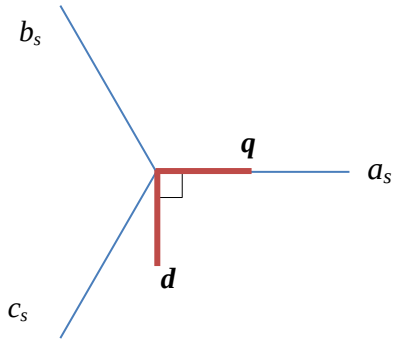

Fig. 11 : stationary qd0 frame

Substitute $\theta = 0$ in (2) results in the stationary transformation given by,

$$T(0) = \frac{2}{3}\begin{bmatrix} 1 & -\frac{1}{2} & -\frac{1}{2} \\ 0 & -\frac{\sqrt{3}}{2} & \frac{\sqrt{3}}{2} \\ \frac{1}{2} & \frac{1}{2} & \frac{1}{2} \end{bmatrix} \quad \textbf{(6)}$$

Then the transformation matrices for the voltage, current and flux linkage of the stator variables could be written as:

$$V_s^{qd0} = T(0)\, V_s^{abc} \quad \textbf{(7)}$$

$$I_s^{qd0} = T(0)\, I_s^{abc} \quad \textbf{(8)}$$

$$\lambda_s^{qd0} = T(0)\, \lambda_s^{abc} \quad \textbf{(9)}$$

On the other hand, the abc vectors of the rotor are rotating making an angle of θ_r with the q vector as shown in Fig. 12:

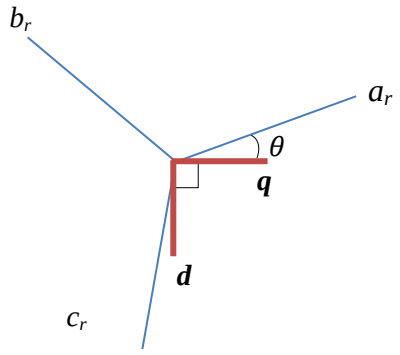

Fig. 12 : abc rotor frame and qd0 frame

Substitute $\theta = -\theta_r$ in (2), yields:

$$T(-\theta_r) = \begin{bmatrix} \cos(\theta_r) & \cos\left(\theta_r + \frac{2\pi}{3}\right) & \cos\left(\theta_r - \frac{2\pi}{3}\right) \\ -\sin(\theta_r) & -\sin\left(\theta_r + \frac{2\pi}{3}\right) & -\sin\left(\theta_r - \frac{2\pi}{3}\right) \\ \frac{1}{2} & \frac{1}{2} & \frac{1}{2} \end{bmatrix} \quad \textbf{(10)}$$

Then the transfer functions for the voltage, current and flux linkage in the stator could be written as:

$$V_r^{qd0} = T(-\theta_r)\, V_r^{abc} \quad \textbf{(11)}$$

$$I_r^{qd0} = T(-\theta_r)\, I_r^{abc} \quad \textbf{(12)}$$

$$\lambda_r^{qd0} = T(-\theta_r)\, \lambda_r^{abc} \quad \textbf{(13)}$$

3. Expanding qd0 transformation to five-phase system

In an N phase system, the transformation will lead to N sequences as explained in [12]. The first sequence is spaced by $\frac{2\pi}{N}$ and the second is spaced by $2 \times \frac{2\pi}{N}$. The final sequence will results in spacing of 2π which means that all phases are in the same direction; this is called the zero sequence.

Thus, a five-phase system will result in five sequences. These five sequences will be spaced by $\frac{2\pi}{5}, \frac{4\pi}{5}, \frac{6\pi}{5}, \frac{8\pi}{5}$ and 2π as shown in Fig. 13.

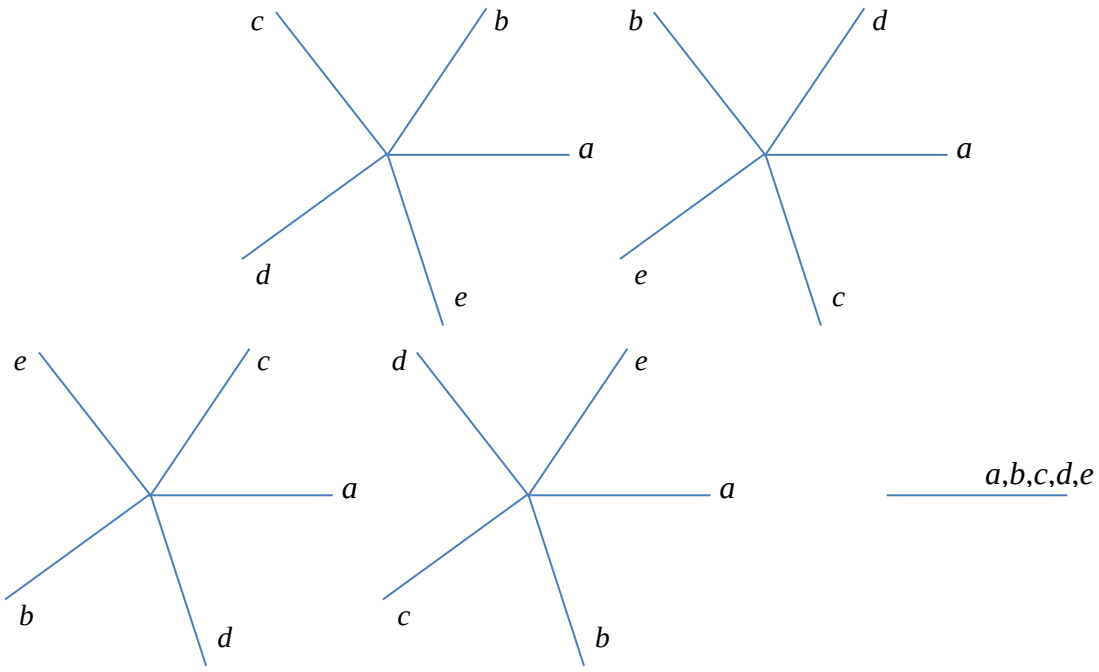

Fig. 13 : Five sequences in five-phase system

It is clear that sequence 1 and 4 are equivalent; same sequence with opposite direction. The same holds true for sequences 2 and 3. Therefore, only sequence 1, 3, and 5 will be used.

Fig. 14 shows the three sequences along with the qd vectors. The first sequence is called q1-q2, the second is q2-d2 and the third is the zero sequence.

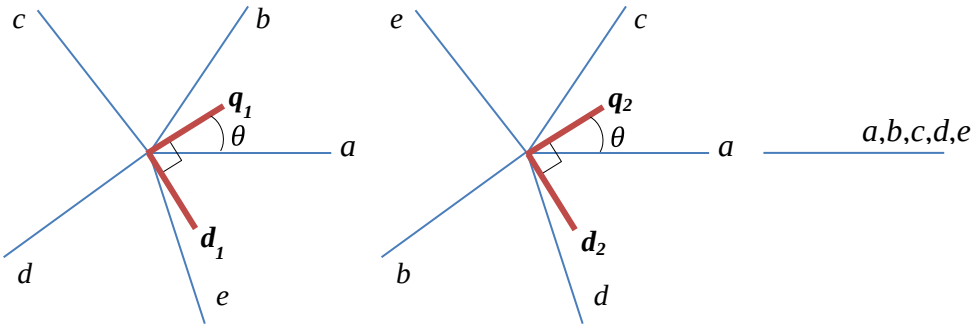

Fig. 14 : q1-d1 and q2-d2 Five Phase System

Using Fig. 14, the following transformation could be derived:

$$\begin{bmatrix} f_{q1} \\ f_{d1} \\ f_{q2} \\ f_{d2} \\ f_0 \end{bmatrix} = \frac{2}{5} \begin{bmatrix} \cos(\theta) & \cos\left(\theta - \frac{2\pi}{5}\right) & \cos\left(\theta - \frac{4\pi}{5}\right) & \cos\left(\theta + \frac{4\pi}{5}\right) & \cos\left(\theta + \frac{2\pi}{5}\right) \\ \sin(\theta) & \sin\left(\theta - \frac{2\pi}{5}\right) & \sin\left(\theta - \frac{4\pi}{5}\right) & \sin\left(\theta + \frac{4\pi}{5}\right) & \sin\left(\theta + \frac{2\pi}{5}\right) \\ \cos(\theta) & \cos\left(\theta + \frac{4\pi}{5}\right) & \cos\left(\theta - \frac{2\pi}{5}\right) & \cos\left(\theta + \frac{2\pi}{5}\right) & \cos\left(\theta - \frac{4\pi}{5}\right) \\ \sin(\theta) & \sin\left(\theta + \frac{4\pi}{5}\right) & \sin\left(\theta - \frac{2\pi}{5}\right) & \sin\left(\theta + \frac{2\pi}{5}\right) & \sin\left(\theta - \frac{4\pi}{5}\right) \\ \frac{1}{2} & \frac{1}{2} & \frac{1}{2} & \frac{1}{2} & \frac{1}{2} \end{bmatrix} \begin{bmatrix} f_a \\ f_b \\ f_c \\ f_d \\ f_e \end{bmatrix}$$

If the other sequences (i.e. 2, 4, and 5) were used, a slightly different but equivalent transformation will be obtained. The inverse of the above transformation is given by:

$$\begin{bmatrix} f_a \\ f_b \\ f_c \\ f_d \\ f_e \end{bmatrix} = \begin{bmatrix} \cos(\theta) & \sin(\theta) & \cos(\theta) & \sin(\theta) & 1 \\ \cos\left(\theta - \frac{2\pi}{5}\right) & \sin\left(\theta - \frac{2\pi}{5}\right) & \cos\left(\theta + \frac{4\pi}{5}\right) & \sin\left(\theta + \frac{4\pi}{5}\right) & 1 \\ \cos\left(\theta - \frac{4\pi}{5}\right) & \sin\left(\theta - \frac{4\pi}{5}\right) & \cos\left(\theta - \frac{2\pi}{5}\right) & \sin\left(\theta - \frac{2\pi}{5}\right) & 1 \\ \cos\left(\theta + \frac{4\pi}{5}\right) & \sin\left(\theta + \frac{4\pi}{5}\right) & \cos\left(\theta + \frac{2\pi}{5}\right) & \sin\left(\theta + \frac{2\pi}{5}\right) & 1 \\ \cos\left(\theta + \frac{2\pi}{5}\right) & \sin\left(\theta + \frac{2\pi}{5}\right) & \cos\left(\theta - \frac{4\pi}{5}\right) & \sin\left(\theta - \frac{4\pi}{5}\right) & 1 \end{bmatrix} \begin{bmatrix} f_{q1} \\ f_{d1} \\ f_{q2} \\ f_{d2} \\ f_0 \end{bmatrix}$$

Stationary qd0 transformation could be obtained by substituting $\theta = 0$ in the above expressions:

$$\begin{bmatrix} f_{q1} \\ f_{d1} \\ f_{q2} \\ f_{d2} \\ f_0 \end{bmatrix} = \frac{2}{5} \begin{bmatrix} 1 & \cos\left(-\frac{2\pi}{5}\right) & \cos\left(-\frac{4\pi}{5}\right) & \cos\left(\frac{4\pi}{5}\right) & \cos\left(\frac{2\pi}{5}\right) \\ 0 & \sin\left(-\frac{2\pi}{5}\right) & \sin\left(-\frac{4\pi}{5}\right) & \sin\left(\frac{4\pi}{5}\right) & \sin\left(\frac{2\pi}{5}\right) \\ 1 & \cos\left(\frac{4\pi}{5}\right) & \cos\left(-\frac{2\pi}{5}\right) & \cos\left(\frac{2\pi}{5}\right) & \cos\left(-\frac{4\pi}{5}\right) \\ 0 & \sin\left(\frac{4\pi}{5}\right) & \sin\left(-\frac{2\pi}{5}\right) & \sin\left(\frac{2\pi}{5}\right) & \sin\left(-\frac{4\pi}{5}\right) \\ \frac{1}{2} & \frac{1}{2} & \frac{1}{2} & \frac{1}{2} & \frac{1}{2} \end{bmatrix} \begin{bmatrix} f_a \\ f_b \\ f_c \\ f_d \\ f_e \end{bmatrix} \qquad \textbf{(14)}$$

4. Properties of the qd0 transformation

In this section, two important properties of the qd0 transformation will be presented. These properties will be used later to derive the model of the induction motor. These two properties are:

$$T(\theta)\frac{d}{dt}T^{-1}(\theta) = \frac{d\theta}{dt}\begin{bmatrix} 0 & 1 & 0 & 0 & 0 \\ -1 & 0 & 0 & 0 & 0 \\ 0 & 0 & 0 & 1 & 0 \\ 0 & 0 & -1 & 0 & 0 \\ 0 & 0 & 0 & 0 & 0 \end{bmatrix} \qquad \textbf{(15)}$$

$$T(\theta)\begin{bmatrix} 1 & \cos\left(\frac{2\pi}{5}\right) & \cos\left(\frac{4\pi}{5}\right) & \cos\left(\frac{4\pi}{5}\right) & \cos\left(\frac{2\pi}{5}\right) \\ \cos\left(\frac{2\pi}{5}\right) & 1 & \cos\left(\frac{2\pi}{5}\right) & \cos\left(\frac{4\pi}{5}\right) & \cos\left(\frac{4\pi}{5}\right) \\ \cos\left(\frac{4\pi}{5}\right) & \cos\left(\frac{2\pi}{5}\right) & 1 & \cos\left(\frac{2\pi}{5}\right) & \cos\left(\frac{4\pi}{5}\right) \\ \cos\left(\frac{4\pi}{5}\right) & \cos\left(\frac{4\pi}{5}\right) & \cos\left(\frac{2\pi}{5}\right) & 1 & \cos\left(\frac{2\pi}{5}\right) \\ \cos\left(\frac{2\pi}{5}\right) & \cos\left(\frac{4\pi}{5}\right) & \cos\left(\frac{4\pi}{5}\right) & \cos\left(\frac{2\pi}{5}\right) & 1 \end{bmatrix} T^{-1}(\theta) = \frac{5}{2}\begin{bmatrix} 1 & 0 & 0 & 0 & 0 \\ 0 & 1 & 0 & 0 & 0 \\ 0 & 0 & 0 & 0 & 0 \\ 0 & 0 & 0 & 0 & 0 \\ 0 & 0 & 0 & 0 & 0 \end{bmatrix} \qquad \textbf{(16)}$$

The derivation could be done using the following basic trigonometric identities.

1. $\sin(\theta)\cos(\theta) = \frac{1}{2}\sin(2\theta)$
2. $\cos^2(\theta) = \frac{1}{2} + \frac{1}{2}\cos(2\theta)$
3. $\sin^2(\theta) = \frac{1}{2} - \frac{1}{2}\cos(2\theta)$
4. $\sin(\alpha + \beta) + \sin(\alpha - \beta) = 2\sin(\alpha)\cos(\beta)$
5. $\cos(\alpha + \beta) + \cos(\alpha + \beta) = 2\cos(\alpha)\cos(\beta)$

CHAPTER III

FIVE PHASE INDUCTION MOTOR MODEL

In this chapter, the model of the five-phase induction motor is derived. The derivation is similar to the three phase case but involve more complex math. The model of five-phase induction motor was first introduced in [13].

1. Voltage, current and flux linkage

In general, five-phase induction motor could be represented as shown in Fig. 15:

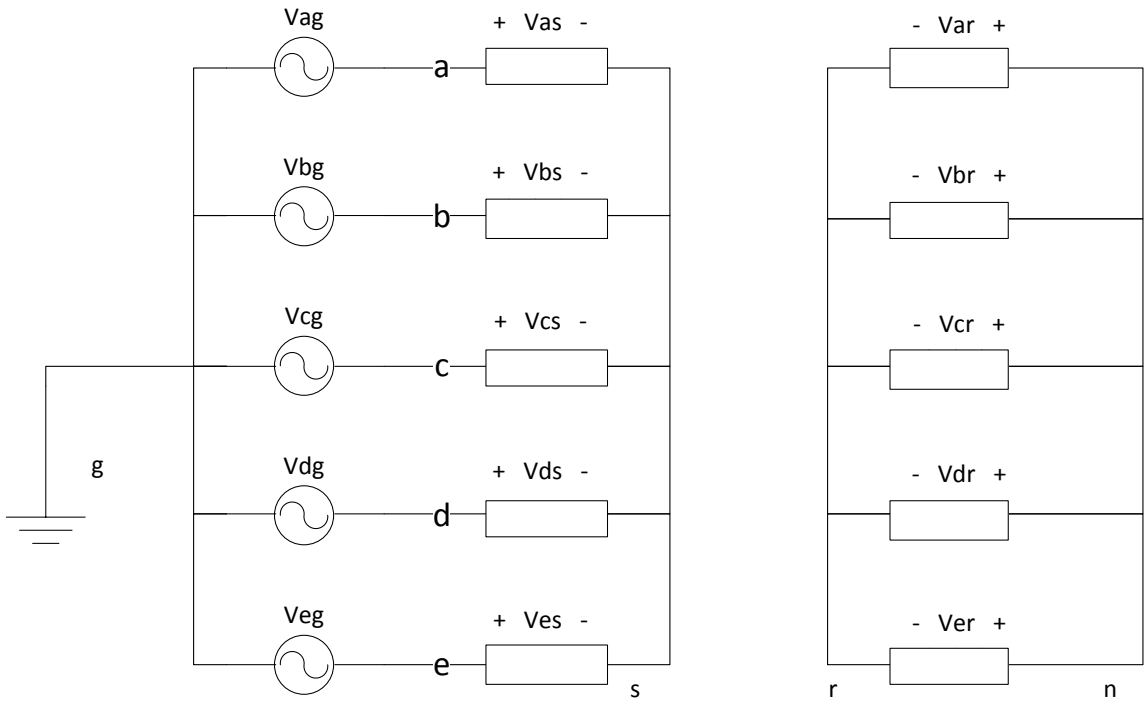

Fig. 15 : Induction motor circuit

Where g is the ground of the input voltage and s is the stator neutral point. To simplify the analysis, the parameters are grouped in vectors as follows:

$$V_g^{abc} = [V_{ag} \quad V_{bg} \quad V_{cg} \quad V_{dg} \quad V_{eg}]^T \tag{17}$$

$$V_s^{abc} = [V_{as} \quad V_{bs} \quad V_{cs} \quad V_{ds} \quad V_{es}]^T \tag{18}$$

$$V_r^{abc} = [V_{ar} \quad V_{br} \quad V_{cr} \quad V_{dr} \quad V_{er}]^T \tag{19}$$

$$I_s^{abc} = [I_{as} \quad I_{bs} \quad I_{cs} \quad I_{ds} \quad I_{es}]^T \tag{20}$$

$$I_r^{abc} = [I_{ar} \quad I_{br} \quad I_{cr} \quad I_{dr} \quad I_{er}]^T \tag{21}$$

$$\lambda_s^{abc} = [\lambda_{as} \quad \lambda_{bs} \quad \lambda_{cs} \quad \lambda_{ds} \quad \lambda_{es}]^T \tag{22}$$

$$\lambda_r^{abc} = [\lambda_{ar} \quad \lambda_{br} \quad \lambda_{cr} \quad \lambda_{dr} \quad \lambda_{er}]^T \tag{23}$$

Where V is the voltage, I is the current and λ is the flux linkage. Subscripts (s) and (r) represent the stator and rotor, respectively. Also define $\mathcal{R}_g$ as the air gap reluctance and n as the turn ratio which is given by:

$$n = \frac{Ns}{Nr} \tag{24}$$

Now defining P as the number of poles, the motor speed is given by:

$$\omega_{rm} = \omega_r \frac{2}{P} \tag{25}$$

Where ω_r is the electrical rotor speed and ω_{rm} is the mechanical rotor speed.

2. Resistances and inductances

In this chapter, r_s and r_r represent the stator and rotor resistances per phase, respectively. Also L_{ls} and L_{lr} are the stator and rotor leakage inductances. Moreover, let L_{ss} be the stator self-inductance and L_{rr} be the rotor self-inductance,

$$L_{ss} = \frac{Ns^2}{\mathcal{R}_g} \quad \text{and} \quad L_{rr} = \frac{Nr^2}{\mathcal{R}_g} \tag{26}$$

L_{sm1}: Mutual inductance between two adjacent stator windings,

$$L_{sm1} = \frac{Ns^2}{\mathcal{R}_g}\cos\left(\frac{2\pi}{5}\right) \tag{27}$$

L_{sm2}: Mutual inductance between two non-adjacent stator windings,

$$L_{sm2} = \frac{Ns^2}{\mathcal{R}_g}\cos\left(\frac{4\pi}{5}\right) \tag{28}$$

L_{rm}: Mutual inductance between rotor windings.

$$L_{rm} = \frac{Nr^2}{\mathcal{R}_g}\cos\left(\frac{2\pi}{5}\right) \tag{29}$$

L_{sr}: Stator to rotor mutual inductance.

$$L_{sr} = \frac{Ns\ Nr}{\mathcal{R}_g} \tag{30}$$

Finally define

$$L_m = \frac{5}{2}L_{ss} \tag{31}$$

Then,

$$L_m = \frac{5}{2}n^2 L_{rr} = \frac{5}{2}nL_{sr} \tag{32}$$

3. abc equations

Stator voltages are given by,

$$\begin{bmatrix} V_{as} \\ V_{bs} \\ V_{cs} \\ V_{ds} \\ V_{es} \end{bmatrix} = r_s \begin{bmatrix} I_{as} \\ I_{bs} \\ I_{cs} \\ I_{ds} \\ I_{es} \end{bmatrix} + \frac{d}{dt} \begin{bmatrix} \lambda_{as} \\ \lambda_{bs} \\ \lambda_{cs} \\ \lambda_{ds} \\ \lambda_{es} \end{bmatrix}$$

Or

$$V_s^{abc} = r_s \, I_s^{abc} + \frac{d}{dt} \lambda_s^{abc} \qquad \textbf{(33)}$$

Rotor voltages are given by,

$$\begin{bmatrix} V_{ar} \\ V_{br} \\ V_{cr} \\ V_{dr} \\ V_{er} \end{bmatrix} = r_r \begin{bmatrix} I_{ar} \\ I_{br} \\ I_{cr} \\ I_{dr} \\ I_{er} \end{bmatrix} + \frac{d}{dt} \begin{bmatrix} \lambda_{ar} \\ \lambda_{br} \\ \lambda_{cr} \\ \lambda_{dr} \\ \lambda_{er} \end{bmatrix}$$

Or

$$V_r^{abc} = r_r \, I_r^{abc} + \frac{d}{dt} \lambda_r^{abc} \qquad \textbf{(34)}$$

Stator flux linkage:

$$\begin{bmatrix}\lambda_{as}\\ \lambda_{bs}\\ \lambda_{cs}\\ \lambda_{ds}\\ \lambda_{es}\end{bmatrix}=\begin{bmatrix}L_{ls}+L_{ss} & L_{sm1} & L_{sm2} & L_{sm2} & L_{sm1}\\ L_{sm1} & L_{ls}+L_{ss} & L_{sm1} & L_{sm2} & L_{sm2}\\ L_{sm2} & L_{sm1} & L_{ls}+L_{ss} & L_{sm1} & L_{sm2}\\ L_{sm2} & L_{sm2} & L_{sm1} & L_{ls}+L_{ss} & L_{sm1}\\ L_{sm1} & L_{sm2} & L_{sm2} & L_{sm1} & L_{ls}+L_{ss}\end{bmatrix}\begin{bmatrix}I_{as}\\ I_{bs}\\ I_{cs}\\ I_{ds}\\ I_{es}\end{bmatrix}$$

$$+L_{sr}\begin{bmatrix}\cos(\theta_r) & \cos\left(\theta_r+\frac{2\pi}{5}\right) & \cos\left(\theta_r+\frac{4\pi}{5}\right) & \cos\left(\theta_r-\frac{4\pi}{5}\right) & \cos\left(\theta_r-\frac{2\pi}{5}\right)\\ \cos\left(\theta_r-\frac{2\pi}{5}\right) & \cos(\theta_r) & \cos\left(\theta_r+\frac{2\pi}{5}\right) & \cos\left(\theta_r+\frac{4\pi}{5}\right) & \cos\left(\theta_r-\frac{4\pi}{5}\right)\\ \cos\left(\theta_r-\frac{4\pi}{5}\right) & \cos\left(\theta_r-\frac{2\pi}{5}\right) & \cos(\theta_r) & \cos\left(\theta_r+\frac{2\pi}{5}\right) & \cos\left(\theta_r+\frac{4\pi}{5}\right)\\ \cos\left(\theta_r+\frac{4\pi}{5}\right) & \cos\left(\theta_r-\frac{4\pi}{5}\right) & \cos\left(\theta_r-\frac{2\pi}{5}\right) & \cos(\theta_r) & \cos\left(\theta_r+\frac{2\pi}{5}\right)\\ \cos\left(\theta_r+\frac{2\pi}{5}\right) & \cos\left(\theta_r+\frac{4\pi}{5}\right) & \cos\left(\theta_r-\frac{4\pi}{5}\right) & \cos\left(\theta_r-\frac{2\pi}{5}\right) & \cos(\theta_r)\end{bmatrix}\begin{bmatrix}I_{ar}\\ I_{br}\\ I_{cr}\\ I_{dr}\\ I_{er}\end{bmatrix}$$

Or,

$$\lambda_s^{abc}=L_{ss}^{abc}\,I_s^{abc}+L_{sr}^{abc}I_r^{abc} \qquad \textbf{(35)}$$

Rotor Flux linkage:

$$\begin{bmatrix}\lambda_{ar}\\ \lambda_{br}\\ \lambda_{cr}\\ \lambda_{dr}\\ \lambda_{er}\end{bmatrix}=L_{sr}\begin{bmatrix}\cos(\theta_r) & \cos\left(\theta_r-\frac{2\pi}{5}\right) & \cos\left(\theta_r-\frac{4\pi}{5}\right) & \cos\left(\theta_r+\frac{4\pi}{5}\right) & \cos\left(\theta_r+\frac{2\pi}{5}\right)\\ \cos\left(\theta_r+\frac{2\pi}{5}\right) & \cos(\theta_r) & \cos\left(\theta_r-\frac{2\pi}{5}\right) & \cos\left(\theta_r-\frac{4\pi}{5}\right) & \cos\left(\theta_r+\frac{4\pi}{5}\right)\\ \cos\left(\theta_r+\frac{4\pi}{5}\right) & \cos\left(\theta_r+\frac{2\pi}{5}\right) & \cos(\theta_r) & \cos\left(\theta_r-\frac{2\pi}{5}\right) & \cos\left(\theta_r-\frac{4\pi}{5}\right)\\ \cos\left(\theta_r-\frac{4\pi}{5}\right) & \cos\left(\theta_r+\frac{4\pi}{5}\right) & \cos\left(\theta_r+\frac{2\pi}{5}\right) & \cos(\theta_r) & \cos\left(\theta_r-\frac{2\pi}{5}\right)\\ \cos\left(\theta_r-\frac{2\pi}{5}\right) & \cos\left(\theta_r-\frac{4\pi}{5}\right) & \cos\left(\theta_r+\frac{4\pi}{5}\right) & \cos\left(\theta_r+\frac{2\pi}{5}\right) & \cos(\theta_r)\end{bmatrix}\begin{bmatrix}I_{as}\\ I_{bs}\\ I_{cs}\\ I_{ds}\\ I_{es}\end{bmatrix}$$

$$+\begin{bmatrix}L_{lr}+L_{rr} & L_{rm} & L_{rm} & L_{rm} & L_{rm}\\ L_{rm} & L_{lr}+L_{rr} & L_{rm} & L_{rm} & L_{rm}\\ L_{rm} & L_{rm} & L_{lr}+L_{rr} & L_{rm} & L_{rm}\\ L_{rm} & L_{rm} & L_{rm} & L_{lr}+L_{rr} & L_{rm}\\ L_{rm} & L_{rm} & L_{rm} & L_{rm} & L_{lr}+L_{rr}\end{bmatrix}\begin{bmatrix}I_{ar}\\ I_{br}\\ I_{cr}\\ I_{dr}\\ I_{er}\end{bmatrix}$$

$$\lambda_r^{abc}=L_{rs}^{abc}\,I_s^{abc}+L_{rr}^{abc}I_r^{abc} \qquad \textbf{(36)}$$

Noting that,

$$L_{sr}^{abc}=[L_{rs}^{abc}]^T$$

4. qd0 equations

A. Stator voltage

The stator voltage vector in the qd0 frame is given by:

$$V_s^{qd0} = T(0)V_s^{abc} = T(0)r_s\, I_s^{abc} + T(0)\frac{d}{dt}\lambda_s^{abc}$$

$$= T(0)r_s\, T^{-1}(0)I_s^{qd0} + T(0)\frac{d}{dt}\left(T^{-1}(0)\lambda_s^{qd0}\right)$$

$$= T(0)\, T^{-1}(0)r_s\, I_s^{qd0} + T(0)\frac{d}{dt}T^{-1}(0)\lambda_s^{qd0} + T(0)T^{-1}(0)\frac{d}{dt}\lambda_s^{qd0}$$

Since $\theta = 0$, then the middle term will be zero:

$$V_s^{qd0} = r_s\, I_s^{qd0} + \frac{d}{dt}\lambda_s^{qd0} \qquad \textbf{(37)}$$

B. Rotor voltage

Similarly,

$$V_r^{qd0} = T(-\theta_r)V_r^{abc} = T(-\theta_r)r_r\, I_r^{abc} + T(-\theta_r)\frac{d}{dt}\lambda_r^{abc}$$

$$= T(-\theta_r)r_r\, T^{-1}(-\theta_r)I_r^{qd0} + T(-\theta_r)\frac{d}{dt}\left(T^{-1}(-\theta_r)\lambda_r^{qd0}\right)$$

$$= T(-\theta_r)\, T^{-1}(-\theta_r)r_r\, I_r^{qd0} + T(-\theta_r)\frac{d}{dt}T^{-1}(-\theta_r)\lambda_r^{qd0}$$

$$+ T(-\theta_r)T^{-1}(-\theta_r)\frac{d}{dt}\lambda_r^{qd0}$$

Again using the property of the transformation with $\theta = -\theta_r \rightarrow \omega = -\omega_r$:

$$V_r^{qd0} = r_r\, I_r^{qd0} + \frac{d}{dt}\lambda_r^{qd0} - \omega_r \begin{bmatrix} 0 & 1 & 0 & 0 & 0 \\ -1 & 0 & 0 & 0 & 0 \\ 0 & 0 & 0 & 1 & 0 \\ 0 & 0 & -1 & 0 & 0 \\ 0 & 0 & 0 & 0 & 0 \end{bmatrix} \lambda_r^{qd0} \qquad \textbf{(38)}$$

C. Stator flux linkage

Using (9) and (35):

$$\lambda_s^{qd0} = T(0)\lambda_s^{abc} = T(0)L_{ss}^{abc}\, I_s^{abc} + T(0)L_{sr}^{abc} I_r^{abc}$$

$$= T(0)L_{ss}^{abc}\, T^{-1}(0) I_s^{qd0} + T(0)L_{sr}^{abc} T^{-1}(-\theta_r) I_r^{qd0}$$

By definition, it could be rewritten as:

$$\lambda_s^{qd0} = L_{ss}^{qd0} I_s^{qd0} + L_{sr}^{qd0} I_r^{qd0} \qquad \textbf{(39)}$$

Where,

$$L_{ss}^{qd0} = T(0)L_{ss}^{abc}\, T^{-1}(0)$$

$$= T(0)\left[(L_{ls}) \begin{bmatrix} 1 & 0 & 0 & 0 & 0 \\ 0 & 1 & 0 & 0 & 0 \\ 0 & 0 & 1 & 0 & 0 \\ 0 & 0 & 0 & 1 & 0 \\ 0 & 0 & 0 & 0 & 1 \end{bmatrix} + L_{ss} \begin{bmatrix} 1 & \cos\left(\frac{2\pi}{5}\right) & \cos\left(\frac{4\pi}{5}\right) & \cos\left(\frac{4\pi}{5}\right) & \cos\left(\frac{2\pi}{5}\right) \\ \cos\left(\frac{2\pi}{5}\right) & 1 & \cos\left(\frac{2\pi}{5}\right) & \cos\left(\frac{4\pi}{5}\right) & \cos\left(\frac{4\pi}{5}\right) \\ \cos\left(\frac{4\pi}{5}\right) & \cos\left(\frac{2\pi}{5}\right) & 1 & \cos\left(\frac{2\pi}{5}\right) & \cos\left(\frac{4\pi}{5}\right) \\ \cos\left(\frac{4\pi}{5}\right) & \cos\left(\frac{4\pi}{5}\right) & \cos\left(\frac{2\pi}{5}\right) & 1 & \cos\left(\frac{2\pi}{5}\right) \\ \cos\left(\frac{2\pi}{5}\right) & \cos\left(\frac{4\pi}{5}\right) & \cos\left(\frac{4\pi}{5}\right) & \cos\left(\frac{2\pi}{5}\right) & 1 \end{bmatrix} \right] T^{-1}(0)$$

Using the properties of qd0 transformation:

$$L_{ss}^{qd0} = L_{ls} \begin{bmatrix} 1 & 0 & 0 & 0 & 0 \\ 0 & 1 & 0 & 0 & 0 \\ 0 & 0 & 1 & 0 & 0 \\ 0 & 0 & 0 & 1 & 0 \\ 0 & 0 & 0 & 0 & 1 \end{bmatrix} + \frac{5}{2} L_{ss} \begin{bmatrix} 1 & 0 & 0 & 0 & 0 \\ 0 & 1 & 0 & 0 & 0 \\ 0 & 0 & 0 & 0 & 0 \\ 0 & 0 & 0 & 0 & 0 \\ 0 & 0 & 0 & 0 & 0 \end{bmatrix} = \begin{bmatrix} L_{ls} + L_m & 0 & 0 & 0 & 0 \\ 0 & L_{ls} + L_m & 0 & 0 & 0 \\ 0 & 0 & L_{ls} & 0 & 0 \\ 0 & 0 & 0 & L_{ls} & 0 \\ 0 & 0 & 0 & 0 & L_{ls} \end{bmatrix}$$

Moreover, using trigonometric identities, it could be shown that

$$L_{sr}^{qd0} = T(0)L_{sr}^{abc} T^{-1}(-\theta_r) = \frac{5}{2} L_{sr} \begin{bmatrix} 1 & 0 & 0 & 0 & 0 \\ 0 & 1 & 0 & 0 & 0 \\ 0 & 0 & 0 & 0 & 0 \\ 0 & 0 & 0 & 0 & 0 \\ 0 & 0 & 0 & 0 & 0 \end{bmatrix}$$

D. Rotor flux linkage

Using (13) and (36):

$$\lambda_r^{qd0} = T(-\theta_r)\lambda_r^{abc} = T(-\theta_r)L_{rs}^{abc}\, I_s^{abc} + T(-\theta_r)L_{rr}^{abc} I_r^{abc}$$

Now using the inverse of (8) and (12):

$$\lambda_r^{qd0} = T(-\theta_r)L_{rs}^{abc}\, T^{-1}(0) I_s^{qd0} + T(-\theta_r)L_{rr}^{abc} T^{-1}(-\theta_r) I_r^{qd0}$$

$$\lambda_r^{qd0} = L_{rs}^{qd0} I_s^{qd0} + L_{rr}^{qd0} I_r^{qd0} \qquad \textbf{(40)}$$

Where,

$$L_{rr}^{qd0} = T(-\theta_r)L_{rr}^{abc}\, T^{-1}(-\theta_r)$$

$$L_{rr}^{qd0} = T(-\theta_r)\left[L_{lr}\begin{bmatrix} 1 & 0 & 0 & 0 & 0 \\ 0 & 1 & 0 & 0 & 0 \\ 0 & 0 & 1 & 0 & 0 \\ 0 & 0 & 0 & 1 & 0 \\ 0 & 0 & 0 & 0 & 1 \end{bmatrix} + L_{rr}\begin{bmatrix} 1 & \cos\left(\frac{2\pi}{5}\right) & \cos\left(\frac{4\pi}{5}\right) & \cos\left(\frac{4\pi}{5}\right) & \cos\left(\frac{2\pi}{5}\right) \\ \cos\left(\frac{2\pi}{5}\right) & 1 & \cos\left(\frac{2\pi}{5}\right) & \cos\left(\frac{4\pi}{5}\right) & \cos\left(\frac{4\pi}{5}\right) \\ \cos\left(\frac{4\pi}{5}\right) & \cos\left(\frac{2\pi}{5}\right) & 1 & \cos\left(\frac{2\pi}{5}\right) & \cos\left(\frac{4\pi}{5}\right) \\ \cos\left(\frac{4\pi}{5}\right) & \cos\left(\frac{4\pi}{5}\right) & \cos\left(\frac{2\pi}{5}\right) & 1 & \cos\left(\frac{2\pi}{5}\right) \\ \cos\left(\frac{2\pi}{5}\right) & \cos\left(\frac{4\pi}{5}\right) & \cos\left(\frac{4\pi}{5}\right) & \cos\left(\frac{2\pi}{5}\right) & 1 \end{bmatrix} \right] T^{-1}(-\theta_r)$$

Again,

$$L_{rr}^{qd0} = L_{lr}\begin{bmatrix} 1 & 0 & 0 & 0 & 0 \\ 0 & 1 & 0 & 0 & 0 \\ 0 & 0 & 1 & 0 & 0 \\ 0 & 0 & 0 & 1 & 0 \\ 0 & 0 & 0 & 0 & 1 \end{bmatrix} + \frac{5}{2}L_{rr}\begin{bmatrix} 1 & 0 & 0 & 0 & 0 \\ 0 & 1 & 0 & 0 & 0 \\ 0 & 0 & 0 & 0 & 0 \\ 0 & 0 & 0 & 0 & 0 \\ 0 & 0 & 0 & 0 & 0 \end{bmatrix} = \begin{bmatrix} L_{lr}+L_m & 0 & 0 & 0 & 0 \\ 0 & L_{lr}+L_m & 0 & 0 & 0 \\ 0 & 0 & L_{lr} & 0 & 0 \\ 0 & 0 & 0 & L_{lr} & 0 \\ 0 & 0 & 0 & 0 & L_{lr} \end{bmatrix}$$

And,

$$L_{rs}^{qd0} = T(-\theta_r)L_{rs}^{abc}T^{-1}(0) = \frac{5}{2}L_{sr}\begin{bmatrix} 1 & 0 & 0 & 0 & 0 \\ 0 & 1 & 0 & 0 & 0 \\ 0 & 0 & 0 & 0 & 0 \\ 0 & 0 & 0 & 0 & 0 \\ 0 & 0 & 0 & 0 & 0 \end{bmatrix}$$

E. Referring rotor parameters to the stator side

Assuming that the turn ratio between stator and rotor is n, then let:

$$V_r^{qd0\prime} = nV_r^{qd0}$$

$$\lambda_r^{qd0\prime} = n\lambda_r^{qd0}$$

$$I_r^{qd0\prime} = I_r^{qd0}/n$$

$$r_r{}' = n^2 r_r$$

$$L_{sr}^{qd0\prime} = nL_{sr}^{qd0}$$

$$L_{rr}^{qd0\prime} = n^2 L_{rr}^{qd0}$$

Then (37),(38),(39) and (40) become:

$$V_s^{qd0} = r_s\, I_s^{qd0} + \frac{d}{dt}\lambda_s^{qd0} \qquad \textbf{(41)}$$

$$V_r^{qd0\prime} = r_r{}'\, I_r^{qd0\prime} + \frac{d}{dt}\lambda_r^{qd0\prime} - \omega_r \begin{bmatrix} 0 & 1 & 0 & 0 & 0 \\ -1 & 0 & 0 & 0 & 0 \\ 0 & 0 & 0 & 1 & 0 \\ 0 & 0 & -1 & 0 & 0 \\ 0 & 0 & 0 & 0 & 0 \end{bmatrix} \lambda_r^{qd0\prime} \qquad \textbf{(42)}$$

$$\lambda_s^{qd0} = L_{ss}^{qd0} I_s^{qd0} + L_{sr}^{qd0\prime} I_r^{qd0\prime} \qquad \textbf{(43)}$$

$$\lambda_r^{qd0\prime} = L_{rs}^{qd0\prime} I_s^{qd0} + L_{rr}^{qd0\prime} I_r^{qd0\prime} \qquad \textbf{(44)}$$

Using (32) the inductance matrices could be written as,

$$L_{sr}^{qd0\prime} = L_{rs}^{qd0\prime} = \begin{bmatrix} L_m & 0 & 0 & 0 & 0 \\ 0 & L_m & 0 & 0 & 0 \\ 0 & 0 & 0 & 0 & 0 \\ 0 & 0 & 0 & 0 & 0 \\ 0 & 0 & 0 & 0 & 0 \end{bmatrix}$$

$$L_{rr}^{qd0} = \begin{bmatrix} L_{lr}{}' + L_m & 0 & 0 & 0 & 0 \\ 0 & L_{lr}{}' + L_m & 0 & 0 & 0 \\ 0 & 0 & L_{lr}{}' & 0 & 0 \\ 0 & 0 & 0 & L_{lr}{}' & 0 \\ 0 & 0 & 0 & 0 & L_{lr}{}' \end{bmatrix}$$

Where $L_{lr}{}' = n^2 L_{lr}$

5. qd0 torque and speed

The input power could be expressed as:

$$P_{in} = V_{as}I_{as} + V_{bs}I_{bs} + V_{cs}I_{cs} + V_{ar}{}'I_{ar}{}' + V_{br}{}'I_{br}{}' + V_{cr}{}'I_{cr}{}'$$

$$P_{in} = \frac{5}{2}V_{q1s}I_{qs} + \frac{5}{2}V_{d1s}I_{ds} + \frac{5}{2}V_{q2s}I_{qs} + \frac{5}{2}V_{d2s}I_{ds} + 5V_{0s}I_{0s}$$

$$+ \frac{5}{2}V_{q1r}{}'I_{qr}{}' + \frac{5}{2}V_{d1r}{}'I_{dr}{}' + \frac{5}{2}V_{q2r}{}'I_{qr}{}' + \frac{5}{2}V_{d2r}{}'I_{dr}{}' + 5V_{0r}{}'I_{0r}{}'$$

Substitute (41) and (42) for the voltages:

$$P_{in} = \frac{5}{2}(r_s{I_{q1s}}^2 + r_s{I_{q2s}}^2 + r_s{I_{d1s}}^2 + r_s{I_{d2s}}^2 + 2r_s{I_{0s}}^2 + r_r{I_{q1r}}'^2 + r_r{I_{d1r}}'^2 + r_r{I_{q2r}}'^2$$

$$+ r_r{I_{d2r}}'^2 + 2r_r{I_{0r}}'^2 + I_{q1s}\frac{d}{dt}\lambda_{q1s} + I_{d1s}\frac{d}{dt}\lambda_{d1s} + I_{q2s}\frac{d}{dt}\lambda_{q2s} + I_{d2s}\frac{d}{dt}\lambda_{d2s}$$

$$+ I_{0s}2\frac{d}{dt}\lambda_{0s} + I_{q1r}{}'\frac{d}{dt}\lambda_{q1r}{}' + I_{d1r}{}'\frac{d}{dt}\lambda_{d1r}{}' + I_{q2r}{}'\frac{d}{dt}\lambda_{q2r}{}' + I_{d2r}{}'\frac{d}{dt}\lambda_{d2r}{}'$$

$$+ I_{0r}{}'2\frac{d}{dt}\lambda_{0r}{}' + \omega_r\lambda_{qr}{}'I_{dr}{}' - \omega_r\lambda_{dr}{}'I_{qr}{}')$$

The power converted to mechanical work is represented by the last two terms only:

$$P_m = \frac{5}{2}\omega_r\left(\lambda_{qr}{}'I_{dr}{}' - \lambda_{dr}{}'I_{qr}{}'\right)$$

$$T_{em} = \frac{P_m}{\omega_{rm}} = \frac{P_m}{\omega_r}\frac{P}{2} = \frac{5}{2}\frac{P}{2}\left(\lambda_{qr}{}'I_{dr}{}' - \lambda_{dr}{}'I_{qr}{}'\right)$$

$$= \frac{5}{2}\frac{P}{2}\left(L_mI_{qs}I_{dr}{}' + (L_m + L_{lr}{}')I_{qr}{}'I_{dr}{}' - L_mI_{ds}I_{qr}{}' - (L_m + L_{lr}{}')I_{dr}{}'I_{qr}{}'\right)$$

$$T_{em} = \frac{5}{2}\frac{P}{2}L_m\left(I_{qs}I_{dr}{}' - I_{ds}I_{qr}{}'\right) \qquad \textbf{(45)}$$

Finally, the speed could be determined as follows:

$$\frac{d}{dt}\omega_{rm} = \frac{1}{J}(T_{em} - T_L)$$

$$\frac{d}{dt}\omega_r = \frac{1}{J}(T_{em} - T_L)\frac{P}{2} \qquad \textbf{(46)}$$

CHAPTER IV

INVERTER MODEL

1. Introduction

Motor drives systems involve two stages between the ac voltage source and the motor. First, the three-phase ac voltage source is converter to dc bus using a rectifier. Then an inverter will convert the dc bus into a controllable three-phase or multiphase ac voltage as desired. Fig. 16 shows a motor drive system with a three-phase output. In this study, the rectifier is assumed to be uncontrollable.

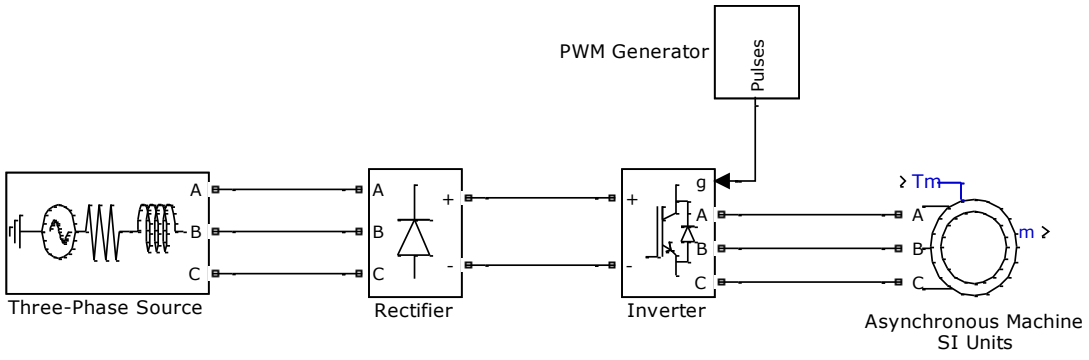

Fig. 16 : Motor Drive System

The two levels inverter consists of six switching devices as shown in Fig. 17.

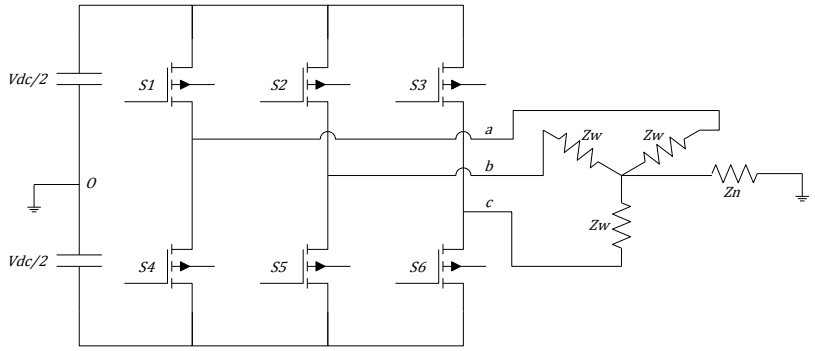

Fig. 17 : Three phase Inveter

The conversion from DC to AC is done by applying the dc bus as pulses to the three phases (a, b, and c). The voltage at each phase is either $+\frac{V_{dc}}{2}$ or $-\frac{V_{dc}}{2}$. By changing the duration of the pulses different phase voltage could be generated. This technique is called pulse width modulation (PWM). It could be done in many ways which may be classified into two main categories:

A. Carrier based PWM

In carrier based PWM the gating signals are generated by comparing the command voltage with a high frequency triangle signal as shown in Fig. 18.

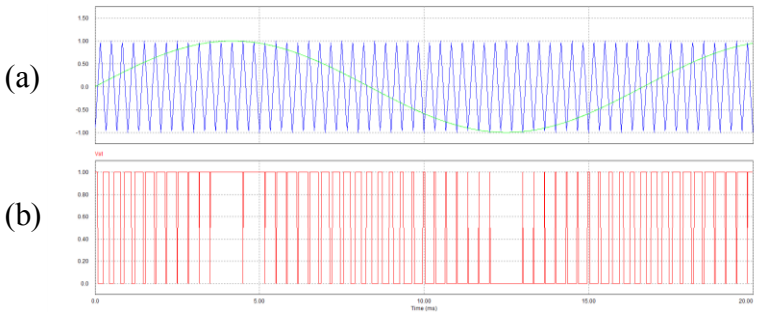

Fig. 18 : Carrier based PWM (a) command and carrier signals (b) output signal

B. Space Vector PWM

In each leg of Fig. 17, if the upper switch is ON then it is marked as 1 and if the lower one is ON it is 0. Space vector pulse width modulation (SVPWM) is a technique where the all of inverter switching possibilities are listed as sets. Each set contains a combination of 1's and 0's that is equal to the number of phases. Thus, the total number of set is given by $2^{\#\text{ of phases}}$. Table 1 shows all the possible combination for three-phase system.

Table 1 : States of the three phase inverter

Switches				Inverter Phase Voltages (x Vdc)				Inverter Line Voltages (x Vdc)		
	S1	S2	S3	Vao	Vbo	Vco	Vo	Vab	Vbc	Vca
0	0	0	0	- 1/2	- 1/2	- 1/2	- 1/2	0	0	0
1	0	0	1	- 1/2	- 1/2	1/2	- 1/6	0	-1	1
2	0	1	0	- 1/2	1/2	- 1/2	- 1/6	-1	1	0
3	0	1	1	- 1/2	1/2	1/2	1/6	-1	0	1
4	1	0	0	1/2	- 1/2	-1/2	- 1/6	1	0	-1
5	1	0	1	1/2	- 1/2	1/2	1/6	1	-1	0
6	1	1	0	1/2	1/2	-1/2	1/6	0	1	-1
7	1	1	1	1/2	1/2	1/2	1/2	0	0	0

Each set could be represented as a vector as shown in Fig. 19. For each of the six sectors, specific vectors are chosen. Afterwards, depending on the required reference voltage, each vector is given a duty ratio such that the average weight of the chosen vectors is equal to the reference voltage.

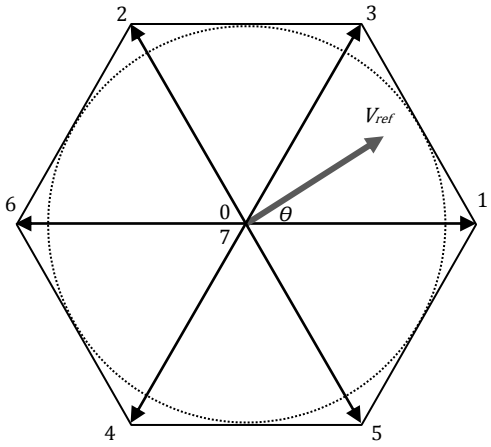

Fig. 19 : Three Phase Space Vector PWM Vectors

In the conventional three-phase switching scheme, the two adjacent vectors and two zero vectors are utilized. For example, in sector 1, vectors 0, 1, 3, and 7 are used such that the average of these four vectors is the reference voltage.

From Table 1, it is clear that the common mode voltage V_o ranges between $-V_{dc}/2$ to $+V_{dc}/2$ and changes in $V_{dc}/3$ steps. A new topology was introduced to eliminate the common mode voltage by adding a fourth leg and a filter to the inverter [14] [15]. These elements will add significant cost to the system. An alternative solution is to modify the switching pattern such that the zero vectors (vectors 0 and 7 in Table 1) are not utilized. This will limit V_o between $-V_{dc}/6$ to $+V_{dc}/6$. Although this will not eliminate V_o it can reduce it significantly. Moreover, the modification is done in the software only and thus no extra cost is added.

Several patterns were introduced to reduce V_o in three-phase inverters. The most successful methods are near-state PWM (NSPWM) and active zero-state PWM1

(AZSPWM1) methods which are discussed in [16]. NSPWM has limited dc bus utilization. In some cases, AZSPWM1 may require that two inverter legs switch simultaneously which is not practical.

2. Five-phase SVPWM

Five-phase SVPWM inverter is similar to the three-phase inverter with extra two legs. Fig. 20 shows the basic configuration of a five-phase inverter.

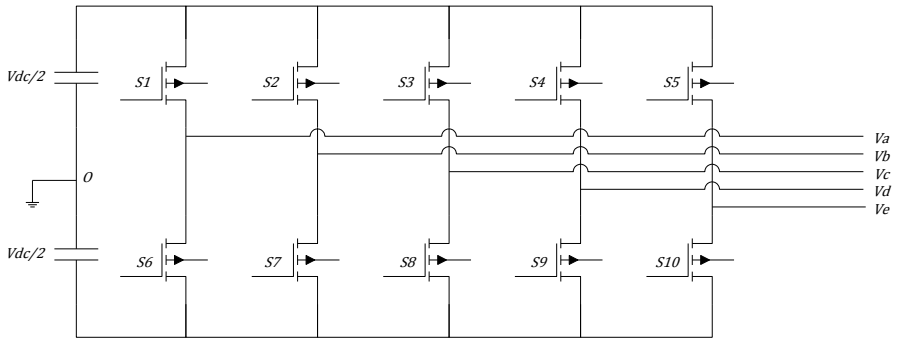

Fig. 20 : Five Phase Inverter

In each leg the top and bottom switches could not be close at the same time since this will short the DC bus. Similar to the three-phase case, each leg is represented as 1 or 0; 1 if the upper switch is ON and 0 if lower one is ON. This will lead to $2^5 = 32$ states which are represented in Table 2.

Moreover, Table 2 shows the resulting phase and line currents for each state. Additionally, it shows the zero sequence voltage which is defined by,

$$V_o = \frac{V_{ao} + V_{bo} + V_{co} + V_{do} + V_{eo}}{5} \qquad \textbf{(47)}$$

Table 2 : States of the five phase inverter

Switches						Inverter Phase Voltages (x VDC)						Inverter Line Voltages (x VDC)				
	S1	S2	S3	S4	S5	Vao	Vbo	Vco	Vdo	Veo	Vo	Vab	Vbc	Vcd	Vde	Vea
0	0	0	0	0	0	- 1/2	- 1/2	- 1/2	- 1/2	- 1/2	-0.5	0	0	0	0	0
1	0	0	0	0	1	- 1/2	- 1/2	- 1/2	- 1/2	1/2	-0.3	0	0	0	-1	1
2	0	0	0	1	0	- 1/2	- 1/2	- 1/2	1/2	- 1/2	-0.3	0	0	-1	1	0
3	0	0	0	1	1	- 1/2	- 1/2	- 1/2	1/2	1/2	-0.1	0	0	-1	0	1
4	0	0	1	0	0	- 1/2	- 1/2	1/2	- 1/2	- 1/2	-0.3	0	-1	1	0	0
5	0	0	1	0	1	- 1/2	- 1/2	1/2	- 1/2	1/2	-0.1	0	-1	1	-1	1
6	0	0	1	1	0	- 1/2	- 1/2	1/2	1/2	- 1/2	-0.1	0	-1	0	1	0
7	0	0	1	1	1	- 1/2	- 1/2	1/2	1/2	1/2	0.1	0	-1	0	0	1
8	0	1	0	0	0	- 1/2	1/2	- 1/2	- 1/2	- 1/2	-0.3	-1	1	0	0	0
9	0	1	0	0	1	- 1/2	1/2	- 1/2	- 1/2	1/2	-0.1	-1	1	0	-1	1
10	0	1	0	1	0	- 1/2	1/2	- 1/2	1/2	- 1/2	-0.1	-1	1	-1	1	0
11	0	1	0	1	1	- 1/2	1/2	- 1/2	1/2	1/2	0.1	-1	1	-1	0	1
12	0	1	1	0	0	- 1/2	1/2	1/2	- 1/2	- 1/2	-0.1	-1	0	1	0	0
13	0	1	1	0	1	- 1/2	1/2	1/2	- 1/2	1/2	0.1	-1	0	1	-1	1
14	0	1	1	1	0	- 1/2	1/2	1/2	1/2	- 1/2	0.1	-1	0	0	1	0
15	0	1	1	1	1	- 1/2	1/2	1/2	1/2	1/2	0.3	-1	0	0	0	1
16	1	0	0	0	0	1/2	- 1/2	- 1/2	- 1/2	- 1/2	-0.3	1	0	0	0	-1
17	1	0	0	0	1	1/2	- 1/2	- 1/2	- 1/2	1/2	-0.1	1	0	0	-1	0
18	1	0	0	1	0	1/2	- 1/2	- 1/2	1/2	- 1/2	-0.1	1	0	-1	1	-1
19	1	0	0	1	1	1/2	- 1/2	- 1/2	1/2	1/2	0.1	1	0	-1	0	0
20	1	0	1	0	0	1/2	- 1/2	1/2	- 1/2	- 1/2	-0.1	1	-1	1	0	-1
21	1	0	1	0	1	1/2	- 1/2	1/2	- 1/2	1/2	0.1	1	-1	1	-1	0
22	1	0	1	1	0	1/2	- 1/2	1/2	1/2	- 1/2	0.1	1	-1	0	1	-1
23	1	0	1	1	1	1/2	- 1/2	1/2	1/2	1/2	0.3	1	-1	0	0	0
24	1	1	0	0	0	1/2	1/2	- 1/2	- 1/2	- 1/2	-0.1	0	1	0	0	-1
25	1	1	0	0	1	1/2	1/2	- 1/2	- 1/2	1/2	0.1	0	1	0	-1	0
26	1	1	0	1	0	1/2	1/2	- 1/2	1/2	- 1/2	0.1	0	1	-1	1	-1
27	1	1	0	1	1	1/2	1/2	- 1/2	1/2	1/2	0.3	0	1	-1	0	0
28	1	1	1	0	0	1/2	1/2	1/2	- 1/2	- 1/2	0.1	0	0	1	0	-1
29	1	1	1	0	1	1/2	1/2	1/2	- 1/2	1/2	0.3	0	0	1	-1	0
30	1	1	1	1	0	1/2	1/2	1/2	1/2	- 1/2	0.3	0	0	0	1	-1
31	1	1	1	1	1	1/2	1/2	1/2	1/2	1/2	0.5	0	0	0	0	0

Using the qd0 transformation presented in Chapter II, these 32 states are represented as vectors on the q1-d1 and q2-d2 frames as shown in Fig. 21.

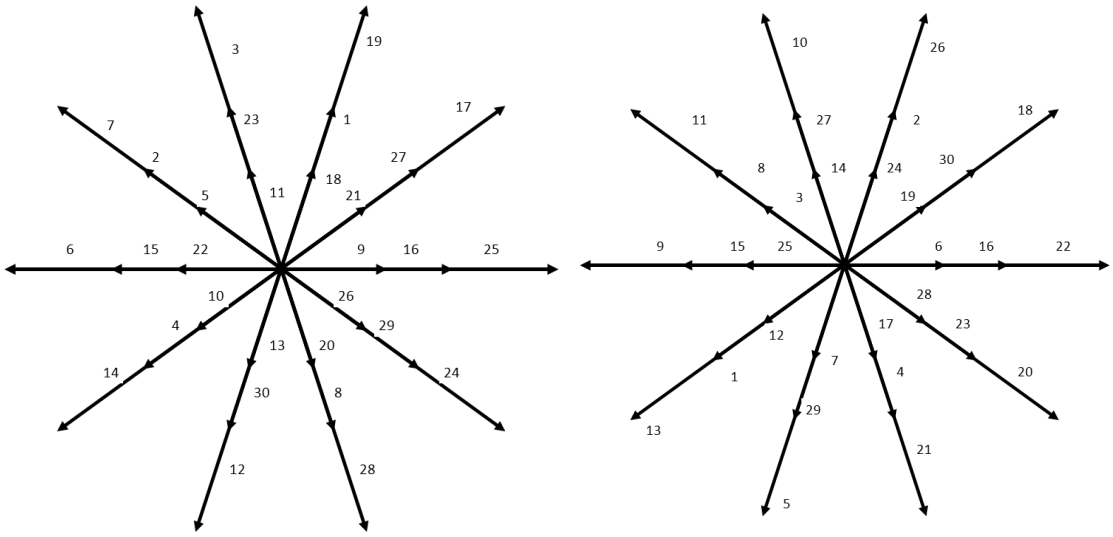

Fig. 21 : The 32 states represented on q1-d1 and q2-d2.

These 32 states could be classified in four categories according to the vector length:

1. 10 Large vectors with length L,
2. 10 Medium vectors with length M,
3. 10 Small vectors with length S,
4. 2 Zero vectors with zero lengths.

Where L, M and S are given by:

$$L = \frac{4}{5} V_{dc} \cos\left(\frac{\pi}{5}\right)$$

$$M = \frac{2}{5} V_{dc} \quad \textbf{(48)}$$

$$S = \frac{4}{5} V_{dc} \cos\left(\frac{2\pi}{5}\right)$$

For a reference voltage with a magnitude V_{ref} and angle θ, the current sector is given by:

$$k = ceil\left(\theta / \frac{\pi}{5}\right) \quad \textbf{(49)}$$

Where $ceil$ represent the round toward positive infinity and:

$$0 \leq \theta < 2\pi \quad \textbf{(50)}$$

Then, V_q and V_d values for the current sector could be calculated as follows:

$$V_q = V_{ref} \cos\left(\theta - (k-1)\frac{\pi}{5}\right) \quad \textbf{(51)}$$

$$V_d = V_{ref} \sin\left(\theta - (k-1)\frac{\pi}{5}\right) \quad \textbf{(52)}$$

Moreover, vectors in each active category (large, medium, and small) will be given specific numbers ranging from 1 to 10. The vectors are numbered with respect to sector in which the reference voltage exists. For instance, Fig. 22(a) shows large vectors numbers with respect to sector 1. It should be noted that the vector numbers are not equivalent to the state values, since the states are constant and do not depend on the sector where the numbers do. Fig. 22(b) represents vector numbers in sector 2. Medium and small vectors are numbered in the exact same way.

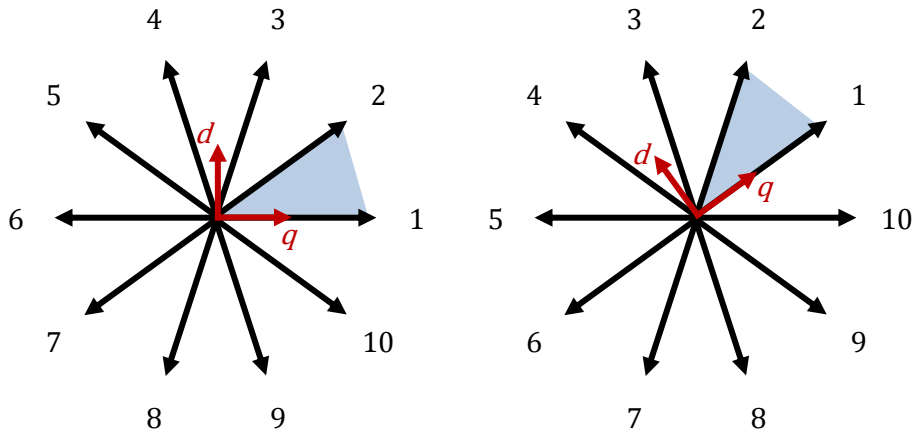

Fig. 22 : Vector Numbers in (a) Sector 1 and (b) Sector 2.

Furthermore, for each of the 30 active vectors, two angels θ_1 and θ_2 are defined. θ_1 is the angel between the vector and the q axis in q1-d1 frame. While θ_2 represents the angel between the vector and the q axis in q2-d2 frame. θ_1 is given by :

$$\theta_1 = (n-1)\frac{\pi}{5} \qquad \textbf{(53)}$$

By comparing Fig. 21(a) and Fig. 21(b), it could be inferred that the direction of large and small vector in q1-d1 frame is mapped to q2-d2 frame in the following direction:

$$\theta_2 = (3n-8k)\frac{\pi}{5} \qquad \textbf{(54)}$$

Where k is the sector number and n is the vector number. With large vectors are mapped as small and vice versa. The direction in which medium vectors are mapped is the opposite of that given in (54):

$$\theta_2 = (3n-8k+5)\frac{\pi}{5} \qquad \textbf{(55)}$$

3. Previously proposed switching patterns

Several Switching Patterns were proposed for the five-phase space vector PWM (SVPWM), Three of them are discussed here:

The first switching pattern is similar to the three phase case [17]; two large (2L) vectors are used along with two zero vectors. Since only two active vectors are used, the average vector in the $q_2 - d_2$ frame could not be controlled. Thus, low order harmonic components are expected.

Another switching pattern which is called (2L+2M) utilizes two large, two medium and two zero vectors [18] [19] [20]. This switching pattern will minimize the switching losses while controlling the $q_2 - d_2$ frame. It only switches 5 times each cycle compared to 7 times in the next switching strategy.

The third one (4L) is where four large vectors and two zero vectors are used [21]. In the last two switching patterns, the two additional vectors allow the control of the q2-d2 frame which reduces the third harmonic and improves the performance.

The three switching patterns were simulated with a five-phase induction motor. The total harmonic distortion THD for each case is shown in Table 3. 4L scheme is shown to have the lowest THD if used with induction motor.

Table 3 : Total harmonic distortion

	No load	**Loaded**
2L	322.2 %	215.8 %
2L+2M	17.48 %	11.74 %
4L	15.20 %	10.23 %

4. Choosing switching vectors

In all previously proposed switching schemes, zero vectors were used. The new switching scheme shall be chosen to reduce the zero sequence voltage V_o. From Table 2, it is obvious that the two zero vectors will produce the highest value of the zero sequence voltage V_o which is $\pm V_{DC}/2$. Additionally, the medium voltages will also produce a relatively high V_o which is $\pm 3\, V_{DC}/10$. Therefore, these vectors are excluded from the new switching topology.

Furthermore, small vectors will map into large vectors in $q_2 - d_2$ frame as shown in Fig. 21. Even if the average of $V_{q2} - V_{d2}$ is kept zero, this will produce larger amount of low order harmonics. Thus, small vectors are also excluded and only large vectors will be used.

Now there are ten large vectors to choose from. In each switching cycle, each one of the chosen vectors will be given a specific duty ratio such that the average of the vectors will equal the reference voltage. As mentioned earlier, V_{q2} and V_{d2} should be zero in order to minimize low order harmonics.

This means that there are five equations to be solved in order to follow the command voltage:

1. V_{q1}^* Equation.
2. V_{d1}^* Equation.
3. $V_{q2}^* = 0$ Equation.
4. $V_{d2}^* = 0$ Equation.
5. The sum of duty ratios shall be equal one.

To solve these five equations, minimum of five vectors are required. Since only large vectors will be used, the pattern will include switching between five large vectors.

Assuming that the chosen vectors are given by (n1, n2, n3, n4, n5) numbers. Then the five equations could be written as:

$$\begin{bmatrix} 1 & 1 & 1 & 1 & 1 \\ L\cos(\theta_1(n_1)) & L\cos(\theta_1(n_2)) & L\cos(\theta_1(n_3)) & L\cos(\theta_1(n_4)) & L\cos(\theta_1(n_5)) \\ L\sin(\theta_1(n_1)) & L\sin(\theta_1(n_2)) & L\sin(\theta_1(n_3)) & L\sin(\theta_1(n_4)) & L\sin(\theta_1(n_5)) \\ S\cos(\theta_2(n_1)) & S\cos(\theta_2(n_2)) & S\cos(\theta_2(n_3)) & S\cos(\theta_2(n_4)) & S\cos(\theta_2(n_5)) \\ S\sin(\theta_2(n_1)) & S\sin(\theta_2(n_2)) & S\sin(\theta_2(n_3)) & S\sin(\theta_2(n_4)) & S\sin(\theta_2(n_5)) \end{bmatrix} \begin{bmatrix} d_1 \\ d_2 \\ d_3 \\ d_4 \\ d_5 \end{bmatrix} = \begin{bmatrix} 1 \\ V_q \\ V_d \\ 0 \\ 0 \end{bmatrix} \quad \textbf{(56)}$$

Where, V_q and V_d are the q and d components of the reference voltage with respect to the current sector. The angles θ_1 and θ_2 are given by (53), (54) and (55). Equation (56) is only valid if vectors (n1, n2, n3, n4, n5) are all large vectors. If medium or small vectors are used the magnitudes and angels should be changed.

If the vectors were chosen, then (56) could be used to calculate duty ratios for any reference voltage. However, the duty ratios should have a positive value. Then, a reference voltage that results in negative values of duty ratios could not be achieved. This means that for a specific set of vectors, not all desired values of V_q and V_d are possible.

For example, Fig. 23(a) shows that reference voltage with small magnitude could not be achieved for a specific switching pattern. Using many variations of the five vectors set, it is shown that the maximum achievable V_q and V_d lies within 85.41 % of the large decagon as shown in Fig. 23(b).

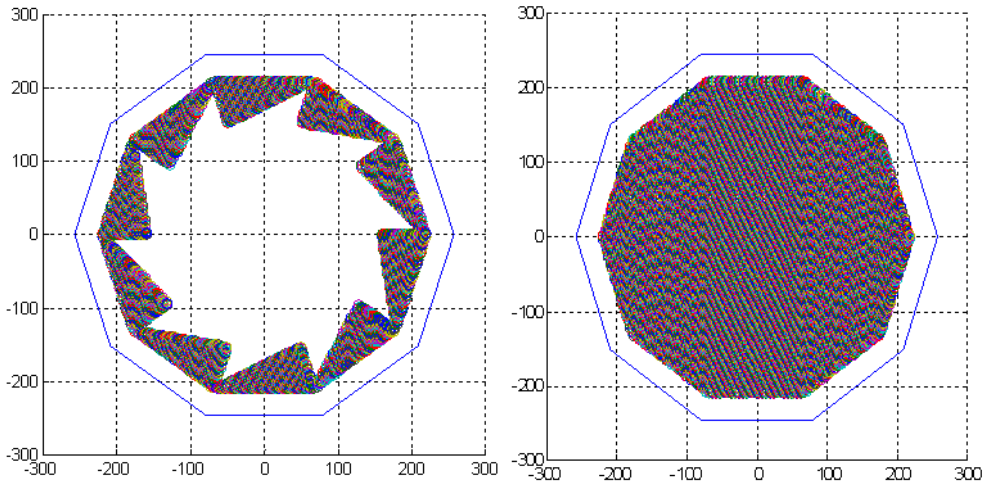

Fig. 23 : (a) Example of achievable range of reference volatge, (b) Maxiumum range of reference voltage.

Where the shaded area represent the area where the required reference voltage is achievable. To achieve the maximum output, the set should include vectors (10, 1, 2 and 3) and exclude vectors (4 and 9). Thus, this will keep only four options:

1. (5L5): vectors 10, 1, 2, 3 and 5.
2. (5L6): vectors 10, 1, 2, 3 and 6.
3. (5L7): vectors 10, 1, 2, 3 and 7.
4. (5L8): vectors 10, 1, 2, 3 and 8.

These four schemes are shown in Fig. 24 for sector 1.

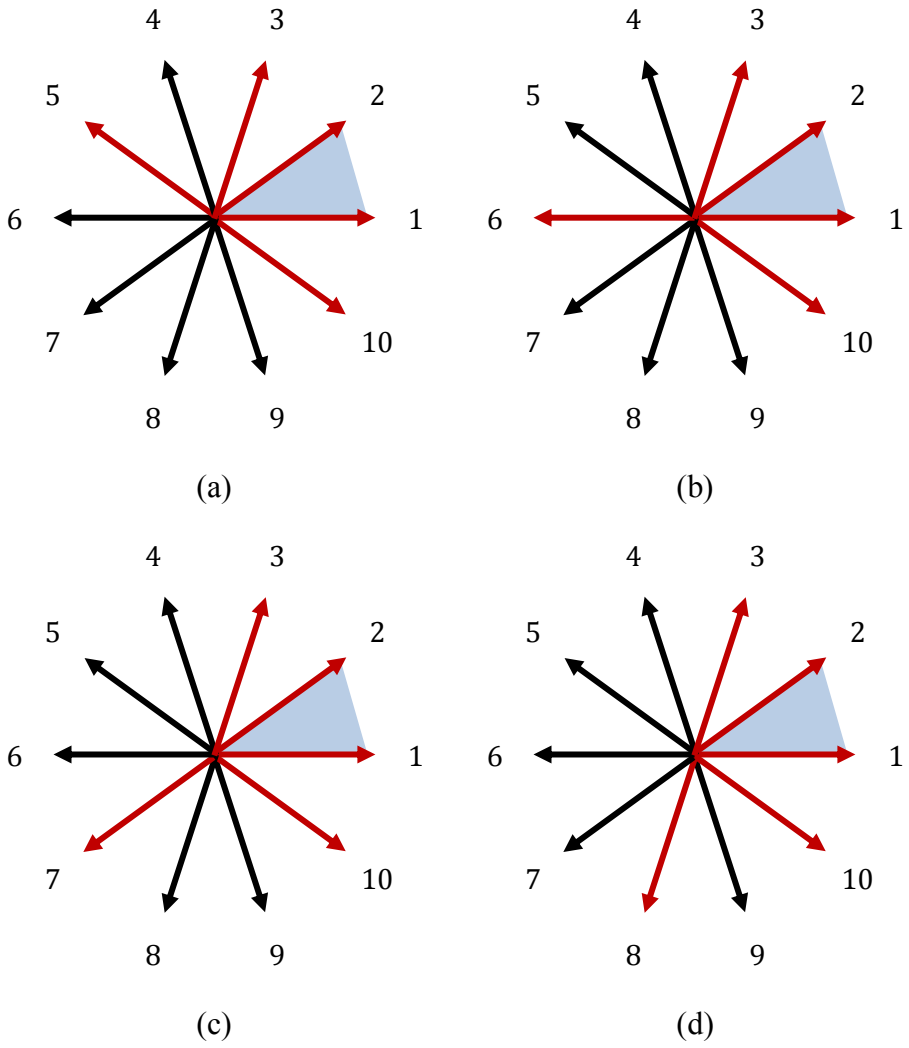

Fig. 24 : (a) 5L5, (b) 5L6, (c) 5L7, (d) 5l8.

In general, the transition from one vector to another adjacent vector requires one switch to be toggled. More switches should toggle if the vector is not adjacent. Each switch change will have some switching losses. For that reason, it is desirable to have a switching pattern with minimum switching changes in one cycle. Table 4 shows the number of switching per cycle for each pattern in symmetrical PWM.

Table 4 : Number of switchings (5L)

	Number of switchings
5L5	5
5L6	6
5L7	6
5L8	5

To compare the performance of the four sets, these sets were simulated in an open loop system and the total harmonic distortion THD is shown in Table 5.

Table 5 : Total harmonic distortion (5L)

	No load	**Loaded**
5L5	20.05 %	17.86 %
5L6	12.89 %	11.39 %
5L7	14.96 %	13.32 %
5L8	18.71 %	16.84 %

It is clear from the table above that the set (5L6) will have the less current THD for both loaded and unloaded case. Thus, among the 5 large vectors schemes, (5L6) represents the best option. In the next section, this switching scheme is implemented.

Moreover, 5L8 shows better performance compared to 5L5 with the same switching losses. For that reason, 5L8 will also be implemented.

5. Implementing 5L6 switching pattern

Now, solving for vectors duty ratios for 5L6 switching pattern using (56):

$$d_6 = \frac{1}{2} - \frac{(5\ c_0 + 15)Vq + (c_1 + 2\ c_2)\ Vd}{2\ V_{dc}\ {c_1}^2}$$

$$d_{10} = \frac{10\ Vq - (3\ c_1 + c_2)\ Vd}{V_{dc}\ {c_1}^2}$$

$$d_1 = \frac{1}{2} + \frac{(5\ c_0 - 25)\ Vq + (c_1 + 2\ c_2)\ Vd}{2\ V_{dc}\ {c_1}^2} \qquad \textbf{(57)}$$

$$d_2 = \frac{10\ Vq + (c_1 - 3\ c_2)\ Vd}{V_{dc}\ {c_1}^2}$$

$$d_3 = \frac{(2\ c_1 + 4\ c_2)\ Vd}{V_{dc}\ {c_1}^2}$$

Where c0, c1, and c2 are three constants defined by:

$$c_0 = \sqrt{5}$$

$$c_1 = 4 \sin\left(\frac{2\pi}{5}\right) = \sqrt{2}\sqrt{5 + \sqrt{5}} \qquad \textbf{(58)}$$

$$c_2 = 4 \sin\left(\frac{\pi}{5}\right) = \sqrt{2}\sqrt{5 - \sqrt{5}}$$

For each switching cycle, every switching device in the inverter will have five states depending on the vectors being used in the current sector. For that reason, for each sector a table representing the exact five vectors is shown in Table 6.

Table 6 : 5L6 switching pattern for each sector

Vector Numbers		6	3	2	1	10	T1	T2
Sector 1	Values	6	19	17	25	24		
	S1	0	1	1	1	1	d1	1
	S2	0	0	0	1	1	d1+d2+d3	1
	S3	1	0	0	0	0	0	d1
	S4	1	1	0	0	0	0	d1+d2
	S5	0	1	1	1	0	d1	d1+d2+d3+d4
Sector 2	Values	14	3	19	17	25		
	S1	0	0	1	1	1	d1+d2	1
	S2	1	0	0	0	1	d1	d1+d2+d3+d4
	S3	1	0	0	0	0	0	d1
	S4	1	1	1	0	0	0	d1+d2+d3
	S5	0	1	1	1	1	d1	1
Sector 3	Values	12	7	3	19	17		
	S1	0	0	0	1	1	d1+d2+d3	1
	S2	1	0	0	0	0	0	d1
	S3	1	1	0	0	0	0	d1+d2
	S4	0	1	1	1	0	d1	d1+d2+d3+d4
	S5	0	1	1	1	1	d1	1
Sector 4	Values	28	6	7	3	19		
	S1	1	0	0	0	1	d1	d1+d2+d3+d4
	S2	1	0	0	0	0	0	d1
	S3	1	1	1	0	0	0	d1+d2+d3
	S4	0	1	1	1	1	d1	1
	S5	0	0	1	1	1	d1+d2	1
Sector 5	Values	24	14	6	7	3		
	S1	1	0	0	0	0	0	d1
	S2	1	1	0	0	0	0	d1+d2
	S3	0	1	1	1	0	d1	d1+d2+d3+d4
	S4	0	1	1	1	1	d1	1
	S5	0	0	0	1	1	d1+d2+d3	1
Sector 6	Values	25	12	14	6	7		
	S1	1	0	0	0	0	0	d1
	S2	1	1	1	0	0	0	d1+d2+d3
	S3	0	1	1	1	1	d1	1
	S4	0	0	1	1	1	d1+d2	1
	S5	1	0	0	0	1	d1	d1+d2+d3+d4
Sector 7	Values	17	28	12	14	6		
	S1	1	1	0	0	0	0	d1+d2
	S2	0	1	1	1	0	d1	d1+d2+d3+d4
	S3	0	1	1	1	1	d1	1
	S4	0	0	0	1	1	d1+d2+d3	1
	S5	1	0	0	0	0	0	d1
Sector 8	Values	19	24	28	12	14		
	S1	1	1	1	0	0	0	d1+d2+d3
	S2	0	1	1	1	1	d1	1
	S3	0	0	1	1	1	d1+d2	1
	S4	1	0	0	0	1	d1	d1+d2+d3+d4
	S5	1	0	0	0	0	0	d1
Sector 9	Values	3	25	24	28	12		
	S1	0	1	1	1	0	d1	d1+d2+d3+d4
	S2	0	1	1	1	1	d1	1
	S3	0	0	0	1	1	d1+d2+d3	1
	S4	1	0	0	0	0	0	d1
	S5	1	1	0	0	0	0	d1+d2
Sector 10	Values	7	17	25	24	28		
	S1	0	1	1	1	1	d1	1
	S2	0	0	1	1	1	d1+d2	1
	S3	1	0	0	0	1	d1	d1+d2+d3+d4
	S4	1	0	0	0	0	0	d1
	S5	1	1	1	0	0	0	d1+d2+d3

To implement the system, two parameters T_1 and T_2 should be defined for each switch (S1, S2, S3, S4 and S5). As shown in Fig. 25, T_1 is the time to switch ON and represent the offset while T_2 is the Time to switch OFF.

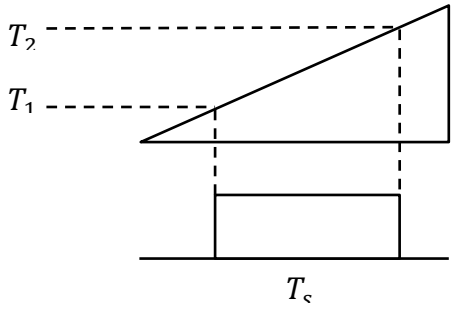

Fig. 25 : Switching Cycle (Mode 1)

As shown in Table 6, in some cases we will have two pulses in one cycle. These cases are marked in red. To implement these cases, the switching control should change such that the first pulse start at zero and ends at T_1. The second pulse will start at T_2 and end at the end of the period as shown in Fig. 26:

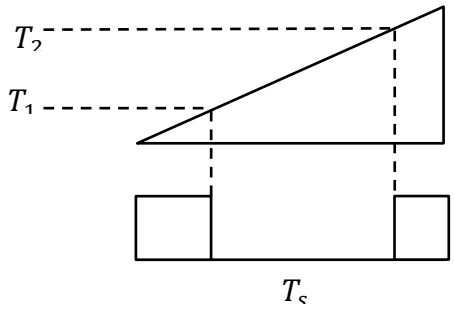

Fig. 26 : Switching Cycle (Mode 2)

6. 6L Switching pattern

As stated earlier, the minimum number of vectors in each switching cycle is five. More vectors could be used but the switching losses should be taken into account. In 5L6 we have relatively high switching losses. Even though there are only five vectors, switching from vector six to ten has a high switching loss. In order to keep the switching losses as low as possible, an additional vector may be used. That is six large vectors with no zero vectors. Using 6 large vectors, five switchings will occur in a cycle. While the 5L6 and 4L will have 6 and 7 switchings, respectively.

If the chosen vectors are 9, 10, 1, 2, 3, and 4, as shown in Fig. 27, then the duty ratio for each vector is derived as follows:

$$d_{4,9} = \frac{1}{2} - \frac{(15 + 5\ c_0)Vq + (c_1 + 2\ c_2)\ V_d}{2\ V_{dc}\ {c_1}^2}$$

$$d_{10} = \frac{10\ Vq - (3\ c_1 + c_2)\ V_d}{V_{dc}\ {c_1}^2}$$

$$d_1 = \frac{(5\ c_0 - 5)Vq + (c_1 + 2c_2)\ V_d}{V_{dc}\ {c_1}^2} \qquad \textbf{(59)}$$

$$d_2 = \frac{10\ Vq + (c_1 - 3\ c_2)\ V_d}{V_{dc}\ {c_1}^2}$$

$$d_3 = \frac{(2\ c_1 + 4\ c_2)\ V_d}{V_{dc}\ {c_1}^2}$$

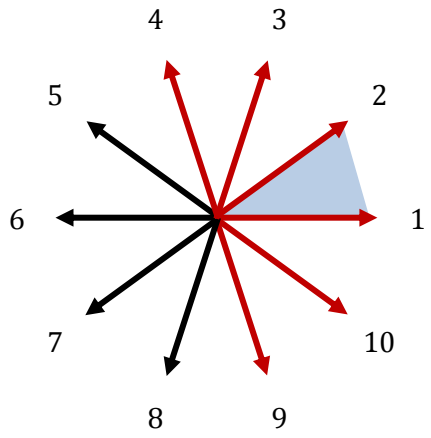

Fig. 27 : 6L switching scheme

The system was simulated and the THD results are shown in Table 7. 6L switching pattern shows an improved performance compared to the case where five or four active vectors are used.

Table 7 : Total harmonic distortion (6L)

	No load	**Loaded**
6L	12.75 %	8.80 %

Table 8 shows 6L Switching Pattern for each sector.

Table 8 : 6L switching pattern for each sector

Vector Numbers		9	10	1	2	3	4	T1	T2
Sector 1	Values	28	24	25	17	19	3		
	S1	1	1	1	1	1	0	0	D5
	S2	1	1	1	0	0	0	0	D3
	S3	1	0	0	0	0	0	0	D1
	S4	0	0	0	0	1	1	D4	1
	S5	0	0	1	1	1	1	D2	1
Sector 2	Values	24	25	17	19	3	7		
	S1	1	1	1	1	0	0	0	D4
	S2	1	1	0	0	0	0	0	D2
	S3	0	0	0	0	0	1	D5	1
	S4	0	0	0	1	1	1	D3	1
	S5	0	1	1	1	1	1	D1	1
Sector 3	Values	25	17	19	3	7	6		
	S1	1	1	1	0	0	0	0	D3
	S2	1	0	0	0	0	0	0	D1
	S3	0	0	0	0	1	1	D4	1
	S4	0	0	1	1	1	1	D2	1
	S5	1	1	1	1	1	0	0	D5
Sector 4	Values	17	19	3	7	6	14		
	S1	1	1	0	0	0	0	0	D2
	S2	0	0	0	0	0	1	D5	1
	S3	0	0	0	1	1	1	D3	1
	S4	0	1	1	1	1	1	D1	1
	S5	1	1	1	1	0	0	0	D4
Sector 5	Values	19	3	7	6	14	12		
	S1	1	0	0	0	0	0	0	D1
	S2	0	0	0	0	1	1	D4	1
	S3	0	0	1	1	1	1	D2	1
	S4	1	1	1	1	1	0	0	D5
	S5	1	1	1	0	0	0	0	D3
Sector 6	Values	3	7	6	14	12	28		
	S1	0	0	0	0	0	1	D5	1
	S2	0	0	0	1	1	1	D3	1
	S3	0	1	1	1	1	1	D1	1
	S4	1	1	1	1	0	0	0	D4
	S5	1	1	0	0	0	0	0	D2
Sector 7	Values	7	6	14	12	28	24		
	S1	0	0	0	0	1	1	D4	1
	S2	0	0	1	1	1	1	D2	1
	S3	1	1	1	1	1	0	0	D5
	S4	1	1	1	0	0	0	0	D3
	S5	1	0	0	0	0	0	0	D1
Sector 8	Values	6	14	12	28	24	25		
	S1	0	0	0	1	1	1	D3	1
	S2	0	1	1	1	1	1	D1	1
	S3	1	1	1	1	0	0	0	D4
	S4	1	1	0	0	0	0	0	D2
	S5	0	0	0	0	0	1	D5	1
Sector 9	Values	14	12	28	24	25	17		
	S1	0	0	1	1	1	1	D2	1
	S2	1	1	1	1	1	0	0	D5
	S3	1	1	1	0	0	0	0	D3
	S4	1	0	0	0	0	0	0	D1
	S5	0	0	0	0	1	1	D4	1
Sector 10	Values	12	28	24	25	17	19		
	S1	0	1	1	1	1	1	D1	1
	S2	1	1	1	1	0	0	0	D4
	S3	1	1	0	0	0	0	0	D2
	S4	0	0	0	0	0	1	D5	1
	S5	0	0	0	1	1	1	D3	1

CHAPTER V

ZERO SEQUENCE CIRCUIT

1. Introduction

In most drive systems, be they three-phase or five-phase, the dc bus is floating. That is, there is no connection between the dc bus terminals and earth. In this case, the dc bus is produced from a rectifier as shown in Fig. 28. The voltage between point o and ground V_{og} has a low magnitude and low frequency compared to the inverter voltages. Thus, it will have no effect on the high frequency circuit. For that reason, V_{og} is neglected and the common mode voltages is referenced to ground instead of point o.

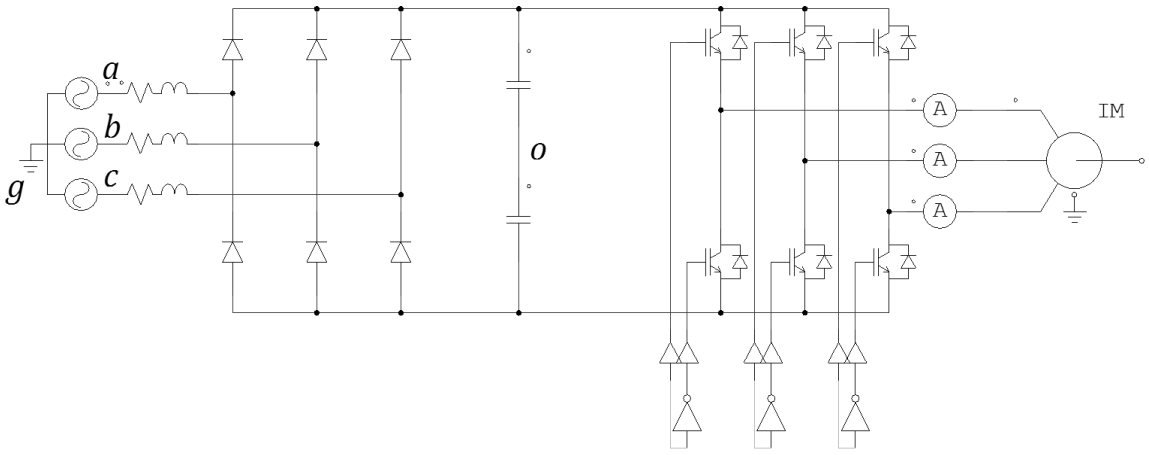

Fig. 28 : Motor drive system

The model of the whole system including the voltage source inverter, the stator windings, and the impedance to ground could be represented by,

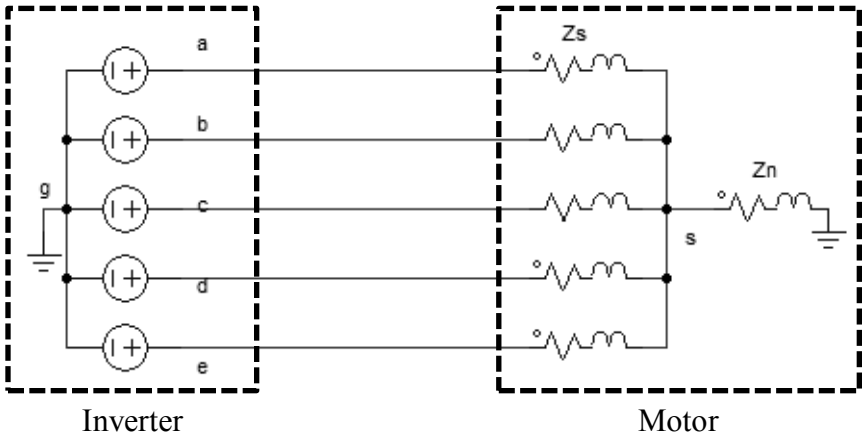

Fig. 29 : Inverter and motor model

From Fig. 29 :

$$\begin{aligned} V_{sg} &= V_{ag} - V_{as} \\ &= V_{bg} - V_{bs} \\ &= V_{cg} - V_{cs} \\ &= V_{dg} - V_{ds} \\ &= V_{eg} - V_{es} \end{aligned} \qquad \textbf{(60)}$$

Adding the above five equations will results in,

$$V_{sg} = \frac{V_{ag} + V_{bg} + V_{cg} + V_{dg} + V_{eg}}{5} - \frac{V_{as} + V_{bs} + V_{cs} + V_{ds} + V_{es}}{5} \qquad \textbf{(61)}$$

Now define,

$$V_{0g} = \frac{V_{ag} + V_{bg} + V_{cg} + V_{dg} + V_{eg}}{5} \qquad \textbf{(62)}$$

$$V_{0s} = \frac{V_{as} + V_{bs} + V_{cs} + V_{ds} + V_{es}}{5} \qquad \textbf{(63)}$$

V_{0g} is called the source common mode voltage and V_{0s} is the load common mode voltage. Then (61) could be written as,

$$V_{sg} = V_{0g} - V_{0s} \quad \textbf{(64)}$$

Using the super position principle on the five sources in

Fig. 29,

$$V_{sg} = \frac{Z_n}{5\,Z_n + Z_s}\left(V_{ag} + V_{bg} + V_{cg} + V_{dg} + V_{eg}\right) = \frac{5\,Z_n}{5\,Z_n + Z_s} V_{0g} \quad \textbf{(65)}$$

Now, Z_s is given by the summation of the input and windings impedance at high frequency,

$$Z_s = Z_{in} + Z_w \quad \textbf{(66)}$$

Using Fig. 7 and Fig. 9 to model Z_n, the above equations could be represented by the zero sequence network shown in Fig. 30,

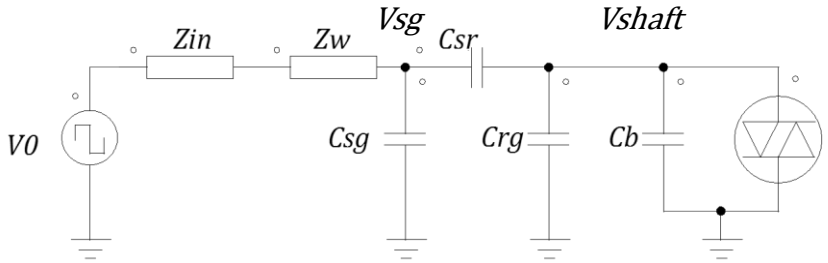

Fig. 30 : Zero sequence circuit

If no breakdown occurs in the bearing capacitance, the circuit could be simplified as shown Fig. 31 where Z_s is modeled as resistance and inductance,

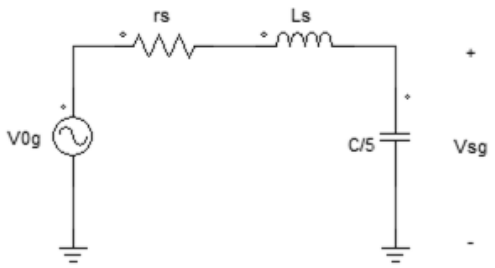

Fig. 31 : Simplified zero sequence circuit

Where C is the equivalent capacitance of the system given by:

$$C = \frac{C_{sr}\left(C_b + C_{rg}\right)}{C_{sr} + C_b + C_{rg}} + C_{sg} \qquad \textbf{(67)}$$

The zero sequence circuit could be used to write the qd0 transformation of the load voltage V_s^{qd0} in terms of the abc source voltage V_g^{abc} rather than the abc load voltage V_s^{abc}. Using the qd0 transformation:

$$V_s^{qd0} = T(0)\, V_s^{abc} = T(0)\begin{bmatrix} V_{ag} - V_{sg} \\ V_{bg} - V_{sg} \\ V_{cg} - V_{sg} \\ V_{dg} - V_{sg} \\ V_{eg} - V_{sg} \end{bmatrix} = T(0)V_g^{abc} - T(0)\begin{bmatrix} 1 \\ 1 \\ 1 \\ 1 \\ 1 \end{bmatrix} V_{sg}$$

Since the summation of the first four rows of $T(0)$ is zero, then the term V_{sg} could be removed.

$$V_s^{qd0} = T(0)V_g^{abc} - \begin{bmatrix} 0 \\ 0 \\ 0 \\ 0 \\ V_{sg} \end{bmatrix} \qquad \textbf{(68)}$$

Where V_{sg} is given by the zero sequence circuit as,

$$V_{sg} = \frac{\frac{5}{L_s\, C}}{s^2 + \frac{r_s}{L_s}s + \frac{5}{L_s\, C}} V_{og} \qquad \textbf{(69)}$$

It is important to evaluate the parameter rs and ls at high frequencies not at 60 Hz. Moreover, the shaft voltage could be derived from Fig. 30 as:

$$V_{shaft} = \frac{C_{sr}}{C_{sr} + C_b + C_{rg}} V_{sg} \qquad \textbf{(70)}$$

This ratio is defined as Bearing Voltage Ratio (BVR):

$$BVR = \frac{V_{shaft}}{V_{sg}} = \frac{C_{sr}}{C_{sr} + C_b + C_{rg}} \qquad \textbf{(71)}$$

Where, the value of BVR ranges between 0 and 1. Furthermore, a new parameter could be defined as Bearing Current Ratio (BCR) which could be derived as:

$$BCR = \frac{I_{bearing}}{I_{0s}} = \frac{C_b}{C}\, BVR \qquad \textbf{(72)}$$

Where, $I_{bearing}$ is the dv/dt part of the bearing current and I_{0s} is the zero sequence current.

2. Step response

Fig. 31 shows the relationship between the voltage at the neutral of the stator V_{sg} and the zero sequence voltage V_{og}. The transfer function is given by:

$$\frac{V_{sg}}{V_{og}} = \frac{\frac{5}{L_s\, C}}{s^2 + \frac{r_s}{L_s}s + \frac{5}{L_s\, C}} = \frac{\omega_n^2}{s^2 + 2\zeta\omega_n s + \omega_n^2} \qquad \textbf{(73)}$$

Where,

$$\omega_n = \sqrt{\frac{5}{L_s\, C}} \quad and \;\; \xi = \frac{r_s}{2}\sqrt{\frac{C}{5\, L_s}} \tag{74}$$

The step response could be derived to be:

$$v_{sg}(t) = V_f + \sqrt{A^2 + B^2}\sin\left(\omega_n t + tan^{-1}\left(\frac{B}{A}\right)\right) \tag{75}$$

The constants A and B depends on the initial conditions $V(0)$ and $\frac{\mathrm{dV(0)}}{\mathrm{dt}}$

$$A = V(0) - V_f$$

$$B = \frac{\frac{dV(0)}{dt} + \frac{r_s}{2L_s}\left(V(0) - V_f\right)}{\omega_n} \tag{76}$$

If the initial condition were set to zero, B will be very small with respect to A. Then the response could be approximated as:

$$v(t) = V_f(1 - \sin(\omega_n t)) \tag{77}$$

Since only large vectors are used, V_f is limited between two values only$\pm\frac{V_{dc}}{10}$ as shown in Table 2. This means that the input of the system will be a positive or negative step with a constant magnitude.

Whenever the input switches to $+\frac{\mathrm{V_{DC}}}{10}$, there will be some negative initial condition. Fig. 32 shows the step response for different initial conditions.

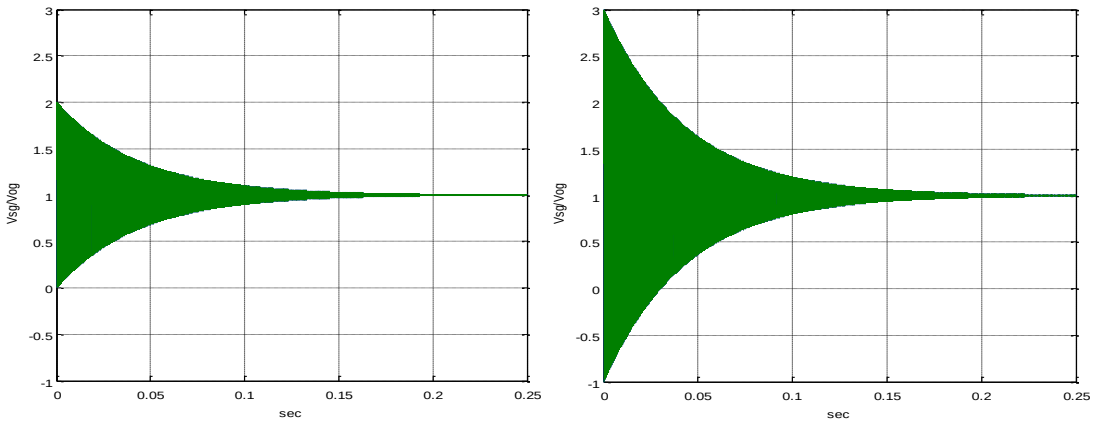

Fig. 32 : Step Response (a) with zero intial condition (b) intial condition = -1

For different motors, the parameters are different. Thus, the switching frequency and damping are dependent on the motor. If the switching frequency is low or the damping is high, the next switching will occur when the response is settled to its final value. Thus, the next switching will start with a negative $\frac{V_{DC}}{10}$ as an initial value.

3. Special case

If the switching frequency is high or damping is very low, the system will appear as an almost undamped system as shown in Fig. 33.

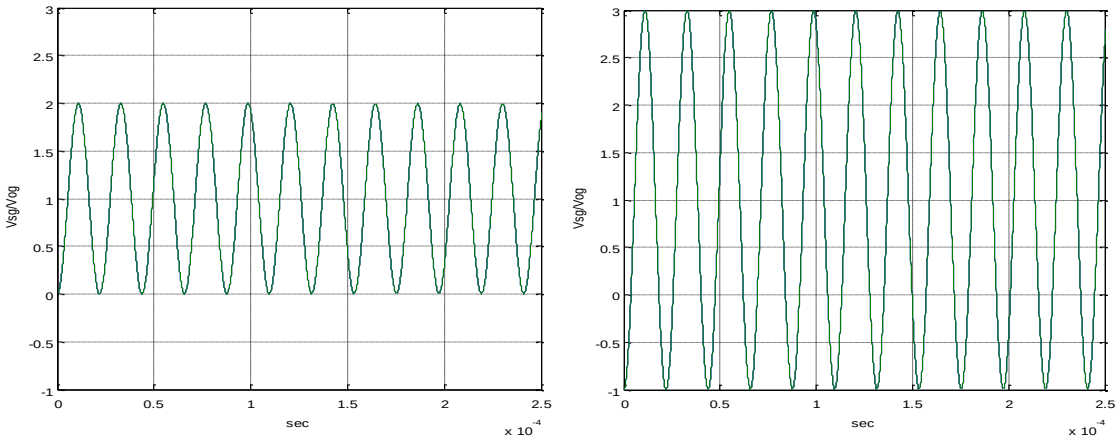

Fig. 33 : Step response, (a) with zero intial condition, (b) intial condition = -1

From Fig. 32 and Fig. 33, it is clear that in order to have minimum response V_{sg}, it is better to switch with initial conditions close to zero. This take place at the bottom critical points of the curve shown in Fig. 33(a) where $V(0)$ is near zero and $\frac{\mathrm{dV(0)}}{\mathrm{dt}} = 0$.

In another words, the best case is to switch at multiples of the natural frequency ω_n. This will ensure that $\frac{\mathrm{dV(0)}}{\mathrm{dt}} = 0$ and $V(0)$ is at minimum value. In this case where the overshoot is around 100%, the response V_{sg} will be almost limited to $\pm \frac{2\mathrm{V_{DC}}}{10}$.

In the case of slow switching, the switching will occurs when $V(0)$ is between 0 and V_f. The worst case will be when $V(0) = -V_f$ which means that V_{sg} will be limited to $\pm \frac{3\mathrm{V_{DC}}}{10}$ in this case.

To put it briefly, if the switching is occurring at multiples of the natural frequency then the voltage at the neutral point of the stator V_{sg} will be a sinusoidal signal

with frequency equals the natural frequency of the system and amplitude limited between $\frac{2V_{DC}}{10}$ and $\frac{3V_{DC}}{10}$ depending on the switching frequency.

To switch at multiples of the natural frequency, the switching frequency should be set to:

$$f_s = \frac{f_n}{n} \quad \textbf{(78)}$$

Where n is an integer.

Moreover, the actual switching is not occurring at f_s only. Because at each switching period, the inverter is switching between five vectors each with specific duty ratio. For that reason, the duty ratios should be set to specific values such that no switching occurs at a fraction of the natural frequency.

If the desired minimum duty ratio is given by the following frequency:

$$f_d = \frac{f_s}{m} \quad \textbf{(79)}$$

Then, after the calculations of the duty ratio values, each value should be rounded to the nearest 1/m value while keeping the sum of the duty ratios equals to one.

CHAPTER VI

SIMULATIONS AND EXPERIMENTAL RESULTS

1. Obtaining zero sequence circuit parameters' values

Fig. 34 presents the zero sequence circuit introduced in Chapter I. Values of the capacitance between stator and ground, stator and rotor, rotor and ground, and the bearing capacitance should be found. The values could be obtained in two ways, calculation or measurement:

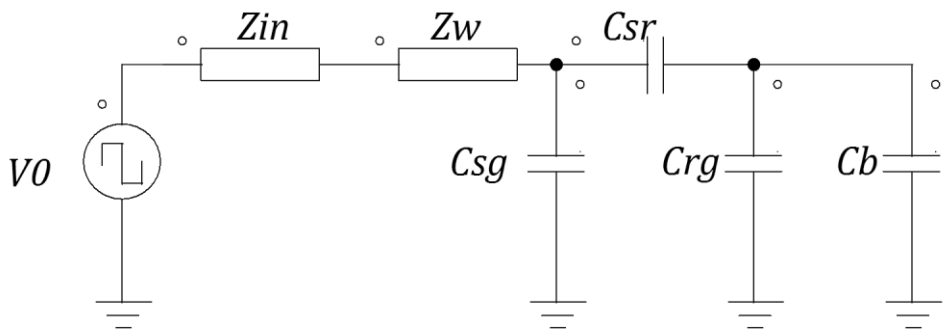

Fig. 34 : Zero sequence Circuit

A. Calculation

To calculate the capacitance values, the basic equation for parallel, cylindrical and spherical capacitor are used [5]:

$$C_{sg} = \frac{K_{sg} N_s \epsilon_r \epsilon_o (W_d + W_s) L_s}{d} \quad \textbf{(80)}$$

$$C_{sr} = \frac{K_{sr} N_r \epsilon_o W_r L_r}{g} \quad \textbf{(81)}$$

$$C_{rg} = \frac{K_{rg}\pi\epsilon_o L_r}{\ln\left(\frac{R_s}{R_r}\right)} \quad \textbf{(82)}$$

$$C_b = \frac{N_b 4\pi\epsilon_r\epsilon_o}{\left(\frac{1}{R_b} - \frac{1}{R_b + R_c}\right)} \quad \textbf{(83)}$$

Where,

- N_s is the number of stator slots.
- N_r is the number of rotor slots.
- N_b is the number of balls.
- ϵ_r is the relative permittivity.
- W_d is the depth of the stator slots.
- W_s is the width of the stator slots.
- W_r is the width of the rotor conductor.
- L_s is the length of the stator.
- L_r is the length of the rotor.
- g is the air gap.
- d is the slot paper thickness.
- R_s is the inside radius of stator.
- R_r is the outer radius of the rotor.
- R_b is the radius of the ball.
- R_c is the radial clearance.

B. Measuring

Measuring the capacitances could be made using an LCR meter. To measure C_{sg} the rotor should be removed to eliminate the effects of other capacitance. C_{sr} is measured by grounding the shaft. After that, the value of C_{sg} is subtracted from the measured reading. To measure C_{rg}, the impedance from rotor to frame is measured, then the effects of C_{sr}, C_b and C_{sg} are subtracted [5].

The results obtained are shown in the following Table.

Table 9 : Parameter values

	Measured Value
C_{sg}	6.498 nF
C_{sr}	0.042 nF
C_{rg}	1.372 nF
C_b	0.350 nF

For these values the expected Bearing Voltage Ratio is:

$$BVR = \frac{V_{sg}}{V_{sg}} = \frac{C_{sr}}{C_{sr} + C_b + C_{rg}} = 0.0238 \qquad \textbf{(84)}$$

This indicates that the shaft voltage is expected to be 2.38% of the stator neutral voltage. If zero vectors are used in the switching pattern, the stator neutral voltage will vary between$\pm\frac{V_{dc}}{2}$. While if no zero vectors were used it will be between $\pm\frac{V_{dc}}{10}$. The shaft voltage will equal the BVR times this voltages.

Next, the circuit is simulated with two cases; with or without zero vectors. For each case, different switching schemes are implemented. The results are shown in the next sections along with the experimental results.

2. Simulation results

The zero sequence circuit was used in the simulation. All the previously mentioned switching schemes were simulated. These include 2L, 2L+2M, 4L, 5L8, 5L6, 6L. The results are shown for both loaded and unloaded cases.

First, the line currents were compared. Table 10 shows the total harmonic distortion THD in line current for these switching schemes.

Table 10 : THD for various switching scheme (simulation)

	No load	**Loaded**
2L	322.2 %	215.8 %
2L+2M	17.48 %	11.74 %
4L	15.20 %	10.23 %
5L6	12.89 %	11.39 %
5L8	18.71 %	16.84 %
6L	12.75 %	8.80 %

Moreover, the neutral point voltage, neutral point current, shaft voltage and bearing current are shown in the following figures for all switching patterns. These results are independent of the motor loading.

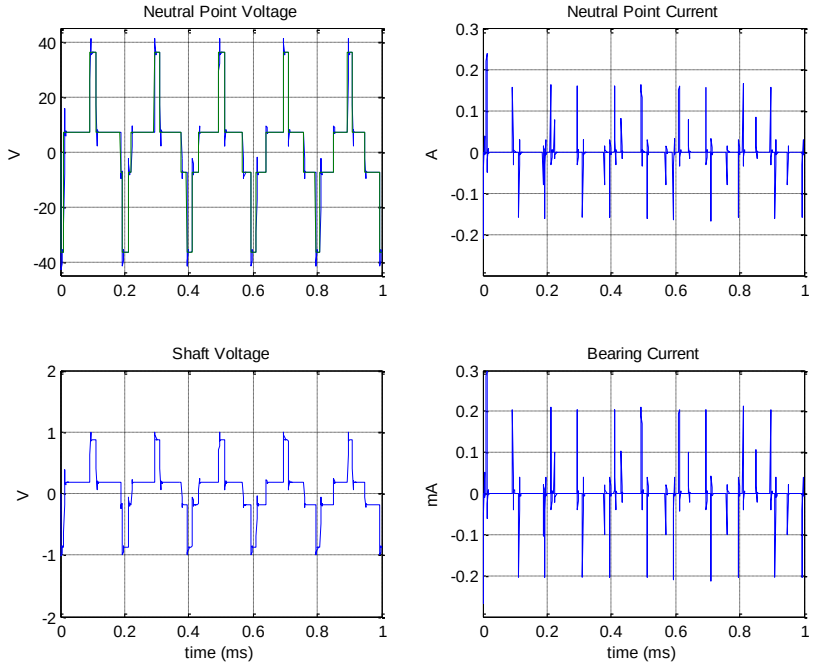

Fig. 35 : (2L) Simulation results

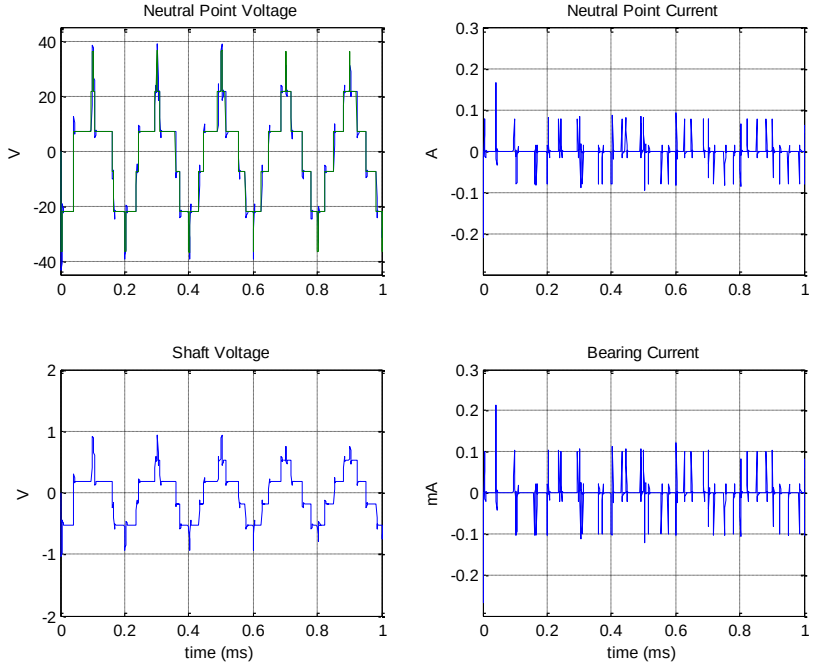

Fig. 36 : (2L+2M) Simulation results

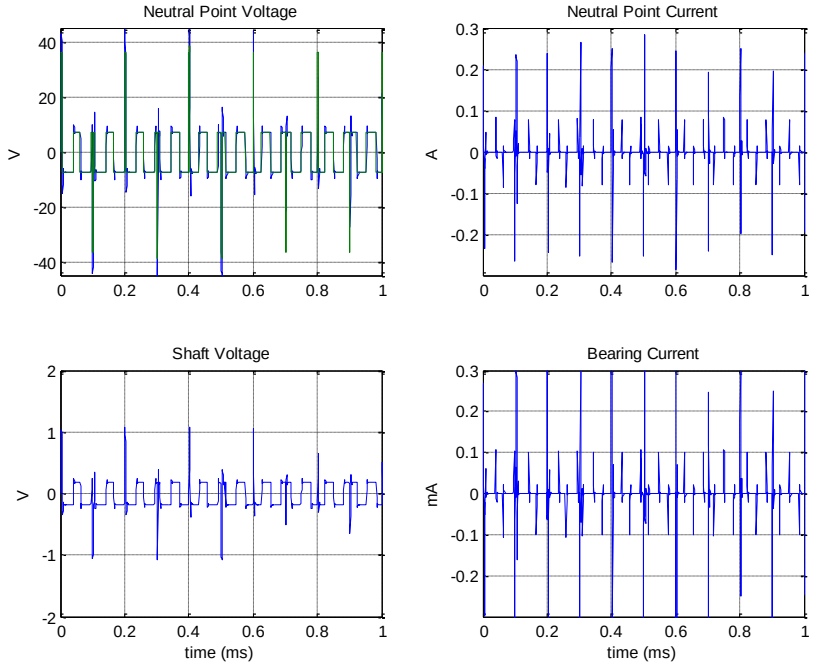

Fig. 37 : (4L) Simulation results

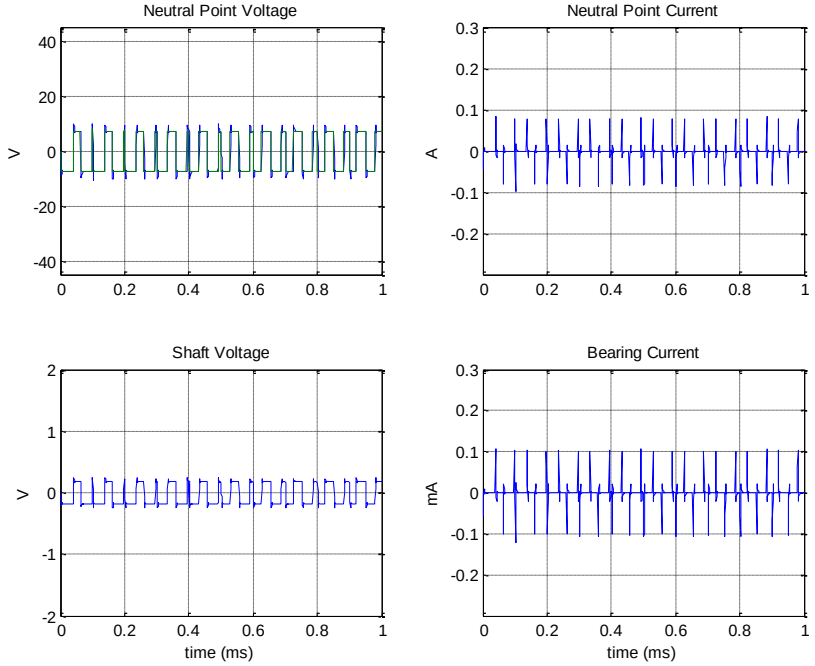

Fig. 38 : (5L8) Simulation results

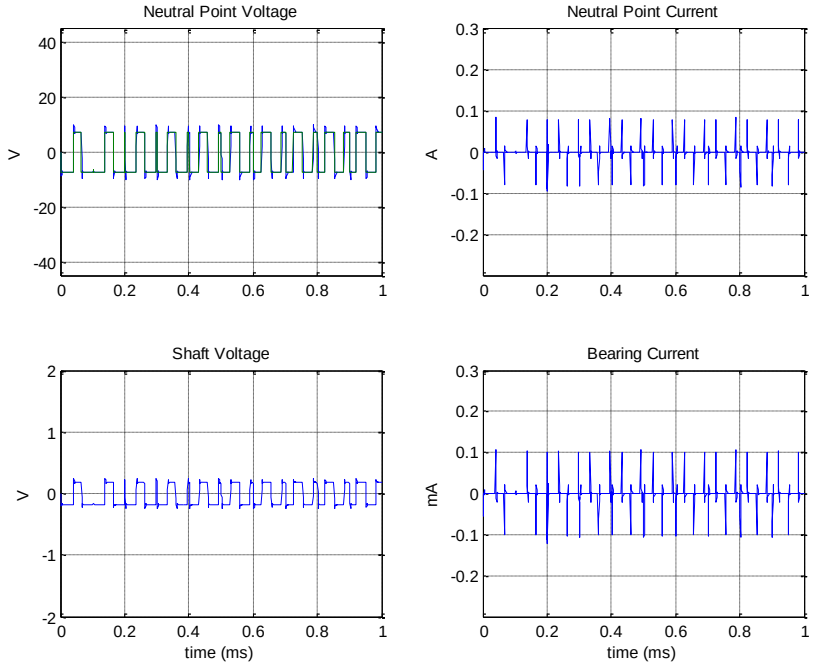

Fig. 39 : (5L6) Simulation results

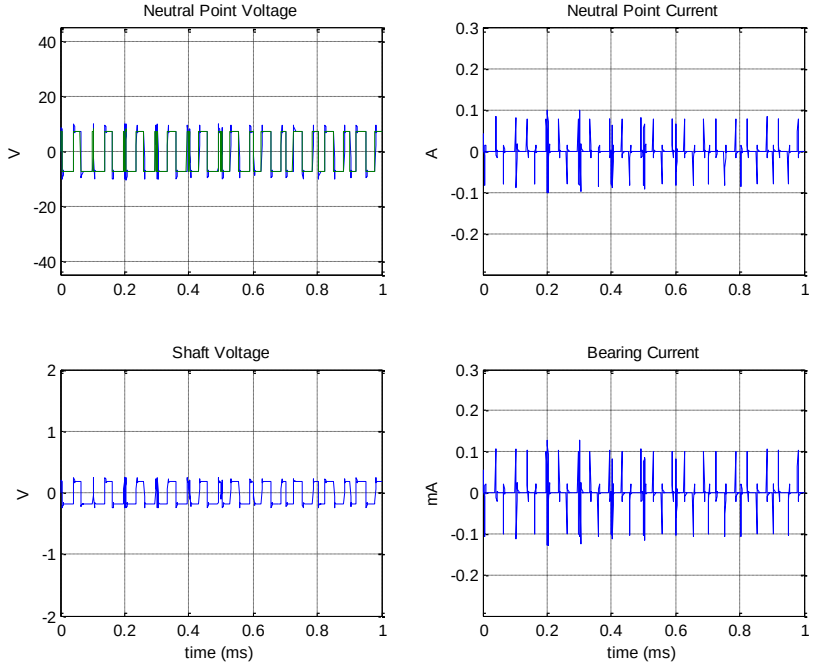

Fig. 40 : (6L) Simulation results

Since the shaft voltage is way below the break down voltage, the current in the previous figures represent only the dv/dt part of the bearing current not the EDM part. dv/dt bearing current does not depend on the magnitude of the shaft voltage but on the rate of change of it. In all switching schemes except 4L the voltage changes in $\frac{V_{dc}}{5}$ steps. Therefore, they will have the same bearing current. 4L have voltage steps of $\frac{2\,V_{dc}}{5}$ and thus has a higher bearing current.

The main advantage of 6L compared to 2L+2M is improving the THD while decreasing the shaft voltage. This will keep the dv/dt bearing current at the same level while decrease the opportunity of EDM bearing currents.

The above results show that the peak value of shaft voltage in 6L is reduced by 5 times as expected. Furthermore, when the zero vectors were used, the rms shaft voltage was 0.872 V while when only large vectors where used it was reduced to 0.193 V. The expected BVR in the simulation is 2.38 %.

3. Experiment setup

Measurement of shaft voltage and bearing current is not an easy procedure. In order to measure shaft voltage, a conductive brush is required. Measuring bearing current is more difficult because there is no access to the current path. For that reason, both bearings should be insulated and a strap should be connected from the outer race to the ground. The current flowing in this strap represents the actual bearing current. Fig. 41 shows the configuration of the motor.

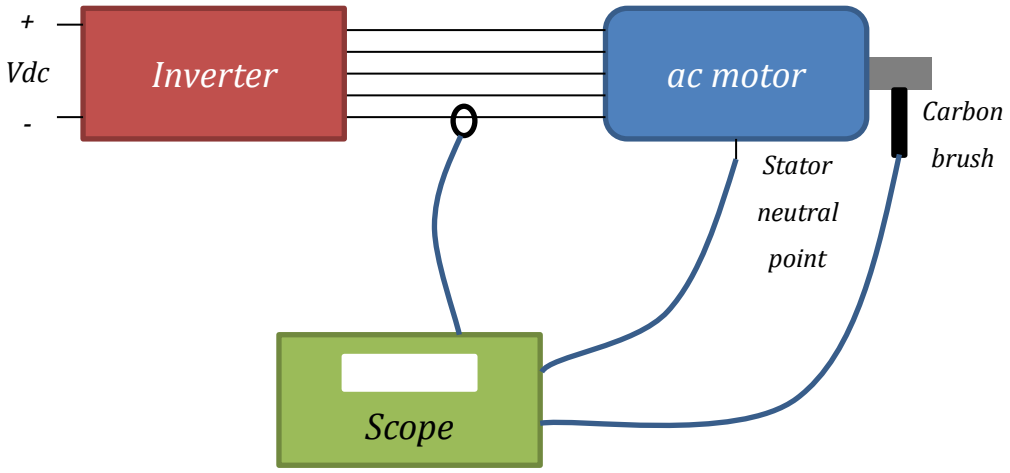

Fig. 41 : Motor configuration.

To generate the PWM pulses, a Texas Instruments Piccolo Microcontroller is used. The TMS320F2803 is 60 MHz device which provides 7 enhanced PWM modules. For each switching strategy, a 'C' Code was written to output the PWM for the five-phase induction motor. Some codes use the zero vectors in the switching pattern, where the others utilize the 5L8, 5L6 and 6L switching pattern with no zero vectors.

The DSP generate the PWM outputs at 3.3 V level. Hence an interface board is required to drive the IGBT at 15 volts level. A 7406 hex inverter driver is used to converts TTL voltage levels to MOS level. Finally, the interface board outputs were connected to 5 IGBT modules to drive the five-phase motor. The switching frequency was chosen to be 10 kHz and dc bus is set to 75 V. The experimental setup is shown in Fig. 42.

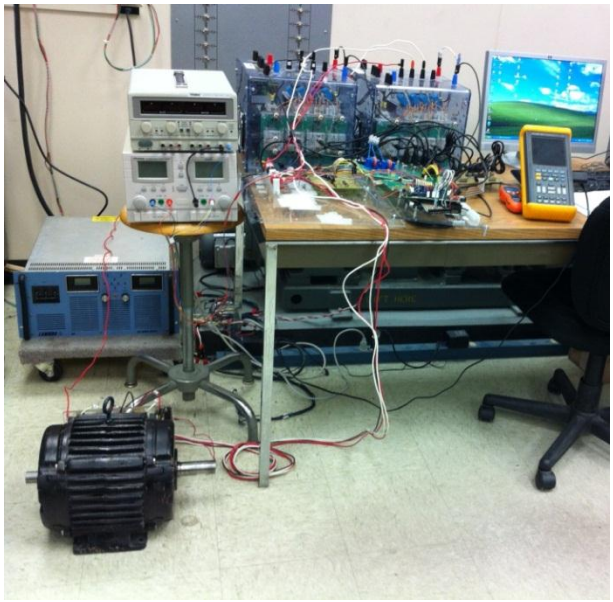

Fig. 42 : Experiment setup

4. Experimental results

All switching schemes were implemented to generate the required gate signals for the IGBT to drive the five-phase induction motor. First the THD in line current was measured and the results are shown in Table 11. 6L pattern shows an improved performance in terms of THD.

Table 11 : THD and current for various switching scheme (experiments)

	No load	
	THD	**rms current**
2L	78.90 %	2.68 A
2L+2M	14.29 %	2.14 A
4L	16.91 %	2.18 A
5L6	12.90 %	2.20 A
5L8	13.34 %	2.22 A
6L	10.37 %	2.26 A

Next, the voltage at the neutral point of the stator was measured. Using a carbon brush the voltage between the motor shaft and frame was measured. Moreover, the zero sequence current was measured. The bearing current could be calculated using the Bearing Current Ratio (BCR). The experimental results are shown in Fig. 43 to Fig. 48. The upper curve is the neutral point voltage and the other one is the shaft voltage.

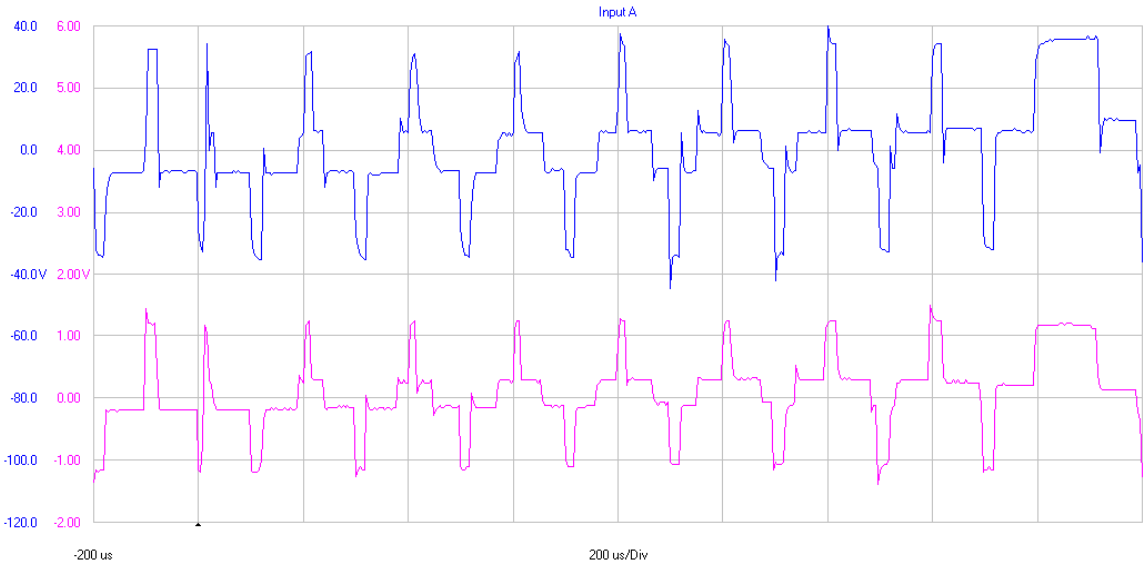

Fig. 43 : (2L) Experimental results

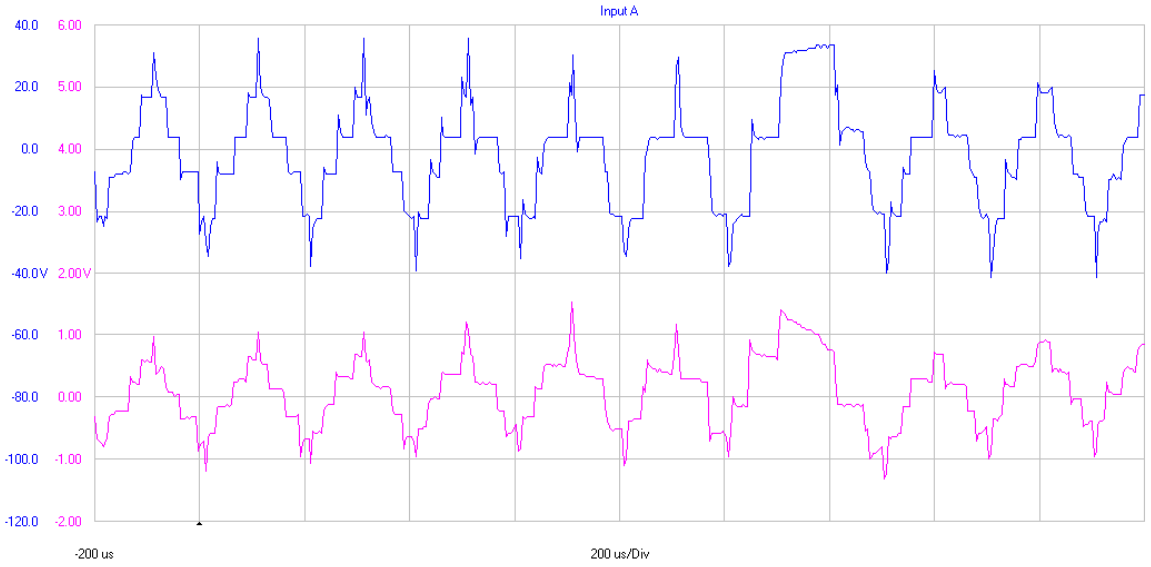

Fig. 44 : (2L+2M) Experimental results

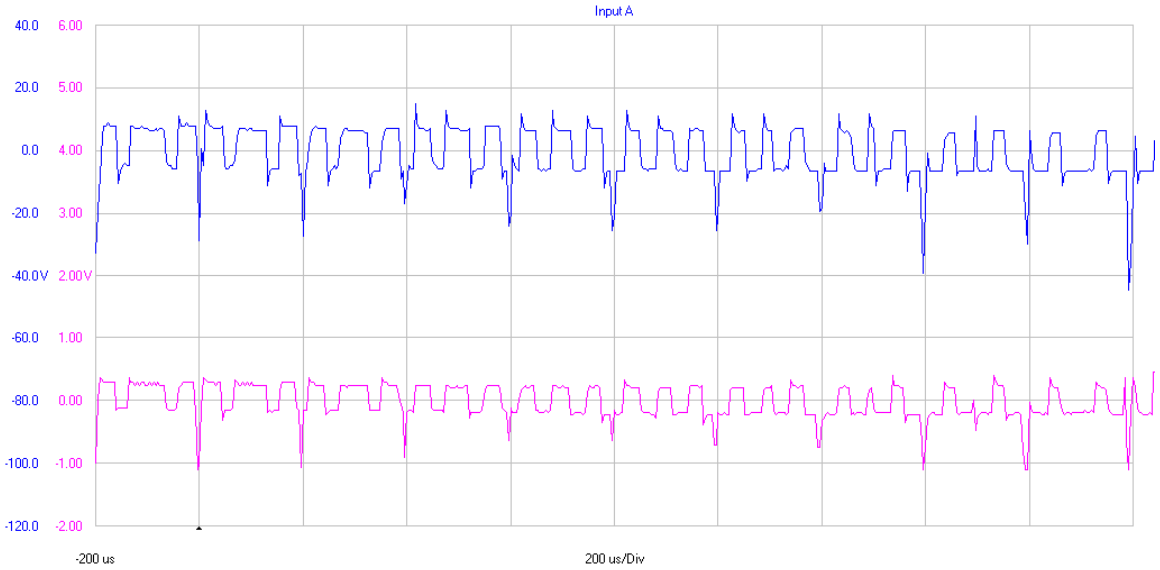

Fig. 45 : (4L) Experimental results

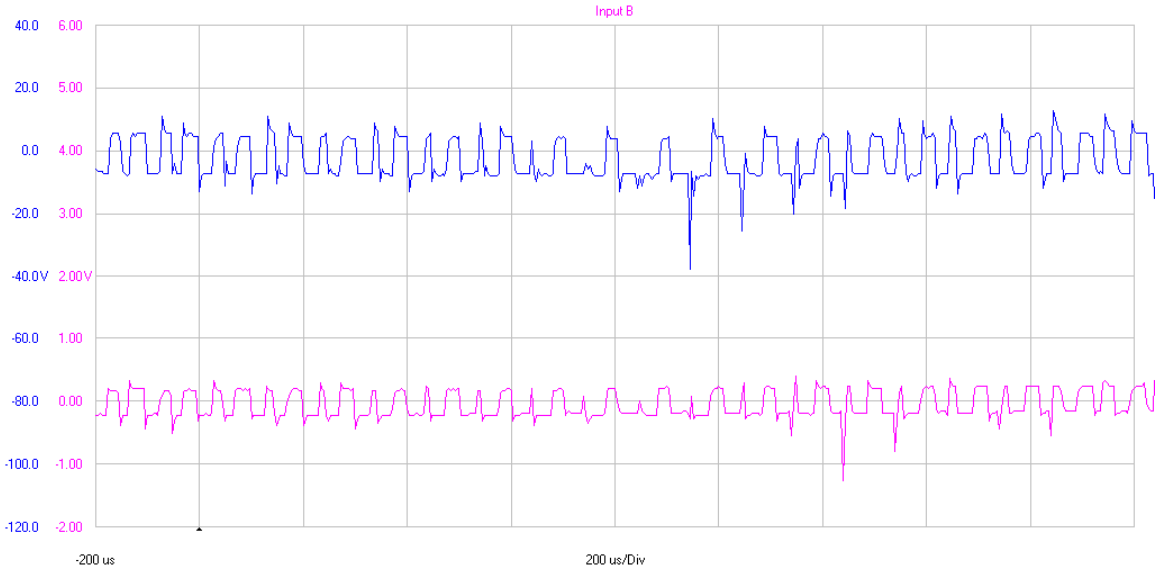

Fig. 46 : (5L6) Experimental results

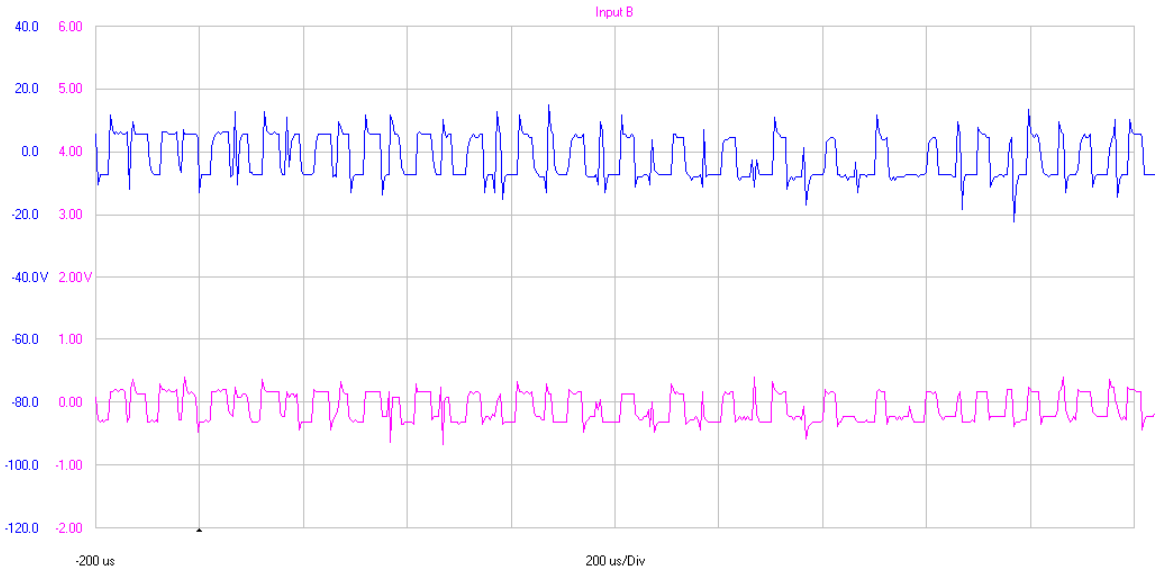

Fig. 47 : (5L8) Experimental results

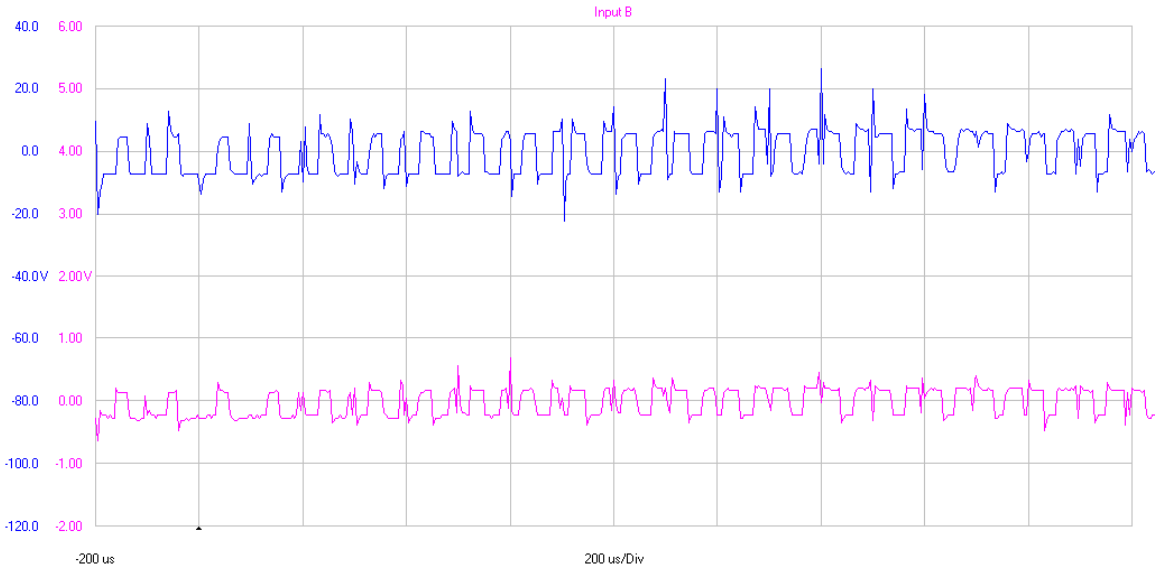

Fig. 48 : (6L) Experimental results

It should be noted that (4L) pattern was employed using one zero vector instead of two. Therefore, the highest value of the neutral point voltage $\frac{V_{dc}}{2}$ does not appear.

The experimental results are shown to be as expected from simulations. Moreover, when the zero vectors were used in (2L+2M), the rms shaft voltage was 0.544 V and the peak was 1.52 V. While when only large vectors where used (6L) rms was reduced to 0.212 V and the peak was 0.680 V. The actual measured Bearing Voltage Ratio (BVR) was 3.24 %.

Furthermore, in (2L+2M) switching pattern, the peak value of the zero sequence current is 0.126 A while in (6L) pattern the peak was reduced to 0.086 A. This may be due to the case where the duty ratio for a vector in (2L+2M) is very short. This may results in switching between two vectors with higher zero sequence voltage difference

which leads to higher dv/dt. This is not the case in (6L) since all vectors have zero sequence voltage between $-V_{dc}/10$ and $+V_{dc}/10$.

Finally, (6L) switching scheme was proven to reduce the shaft voltage to 20% of the original value. Depending on the system voltage levels and the break down voltage, this may eliminate the EDM bearing currents.

5. Current regulation

The goal of this work is to minimize the voltage at the neutral point of the stator while keeping the line currents at a sinusoidal shape with minimum amount of harmonics. In five-phase machines, the required sinusoidal currents are shifted by 72^{o} degrees. Transforming these current to qd0 frame using:

$$I^{qd0} = T(\theta)I^{abc} \quad \textbf{(85)}$$

Will result in:

$$\begin{aligned} I_{q1} &= |I|\cos(\theta) \\ I_{d1} &= |I|\sin(\theta) \\ I_{q2} &= I_{d2} = I_o = 0 \end{aligned} \quad \textbf{(86)}$$

In closed loop system, two command currents are specified for Iq and Id in the rotating reference frame. To force the currents to follow the commands, two PI controllers are used as shown in Fig. 49.

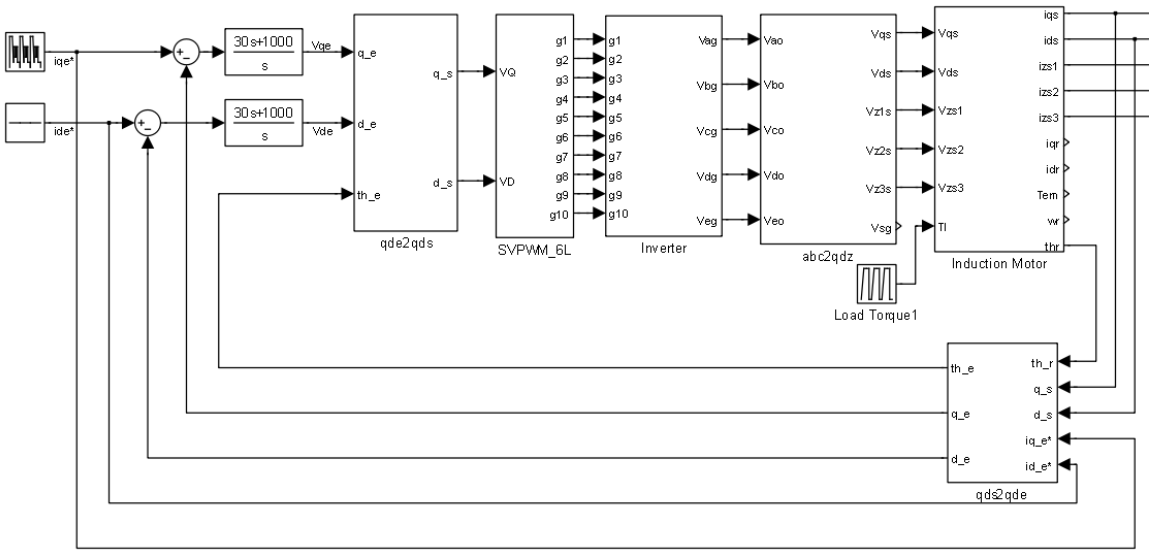

Fig. 49 : Current Regulated SVPWM

In this system, I_{q2}, I_{d2} and I_o were not fed back. It is enough to set the corresponding command voltages V_{q2}, V_{d2} and V_o to zero. This will insure minimizing these currents because each of them is related to its voltage by the following transfer function as shown in Chapter IV:

$$I = \frac{1}{r_s + s\,L_s} V \qquad \textbf{(87)}$$

The e2s and s2e blocks shown in Fig. 49 transform I_q and I_d from the stationary frame to the rotating frame. Fig. 50 shows the relation between these two frames.

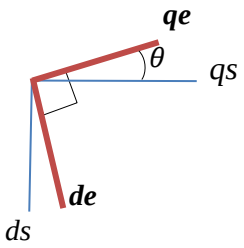

Fig. 50 : Stationary and rotating refrence frames.

The angle θ is given by [22]:

$$\theta = \theta_r + \theta_2 \quad \textbf{(88)}$$

$$\theta_2 = \frac{I_q^*}{I_d^*} \frac{r_r}{s\, l_r} \quad \textbf{(89)}$$

Where θ_r is the rotor angle and θ_2 is the compensated slip angle. The s2e transformation is given by,

$$\begin{aligned} q_e &= q_s \cos(\theta) - d_s \sin(\theta) \\ d_e &= q_s \sin(\theta) + d_s \cos(\theta) \end{aligned} \quad \textbf{(90)}$$

Whereas e2s transformation is,

$$\begin{aligned} q_s &= q_e \cos(\theta) + d_e \sin(\theta) \\ d_s &= -q_e \sin(\theta) + d_e \cos(\theta) \end{aligned} \quad \textbf{(91)}$$

6. Comparing (6L) with (2L+2M) under CRPWM

In this section, the (6L) sequence which includes six large vectors with no zero vectors is compared with (2L+2M) sequence which has two large, two medium and two zero vectors. The simulation is done with Current Regulated PWM (CRPWM) to show the ability of the new switching pattern to follow the commanded currents.

The simulation results for the (2L+2M) sequence are shown in Fig. 51. Fig. 51(a) and (b) show Iq and Id respectively. Fig. 51(c) shows the stator currents. The torque and speed are presented in Fig. 51(d) and (e). Similarly, Fig. 52 shows the simulation results for (6L) sequence.

It is clear from the figures that (6L) sequence will have almost equivalent Iq, Id, line currents, torque, speed, and THD. The only difference is that (6L) will have higher Iq and Id current ripple. Moreover, (6L) reduces the neutral voltage and current which will reduce the shaft voltage and bearing current.

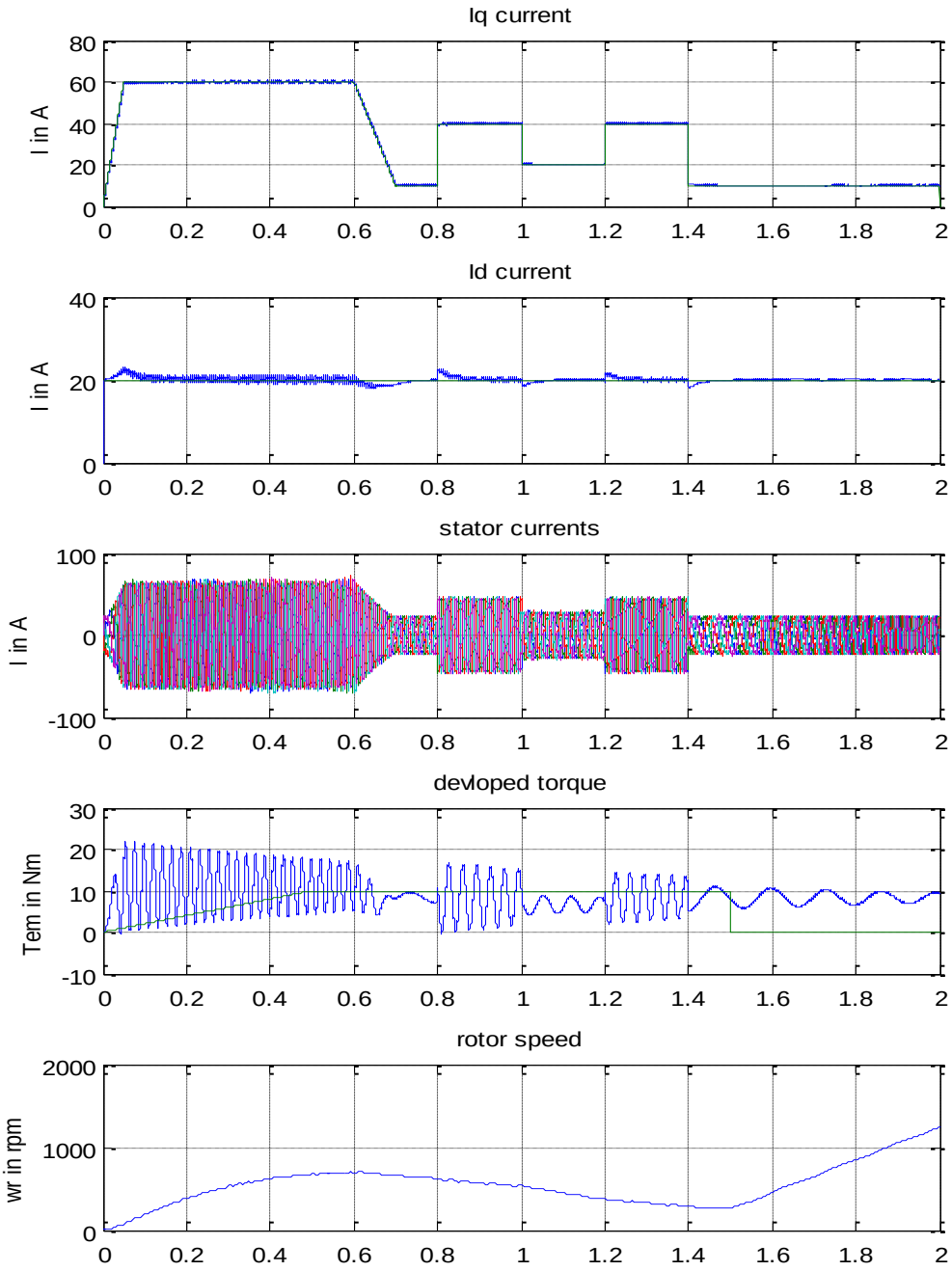

Fig. 51 : 2L+2M Sequence (a) Iq (b) Id (c) Stator Currents (d) Torque (e) Speed

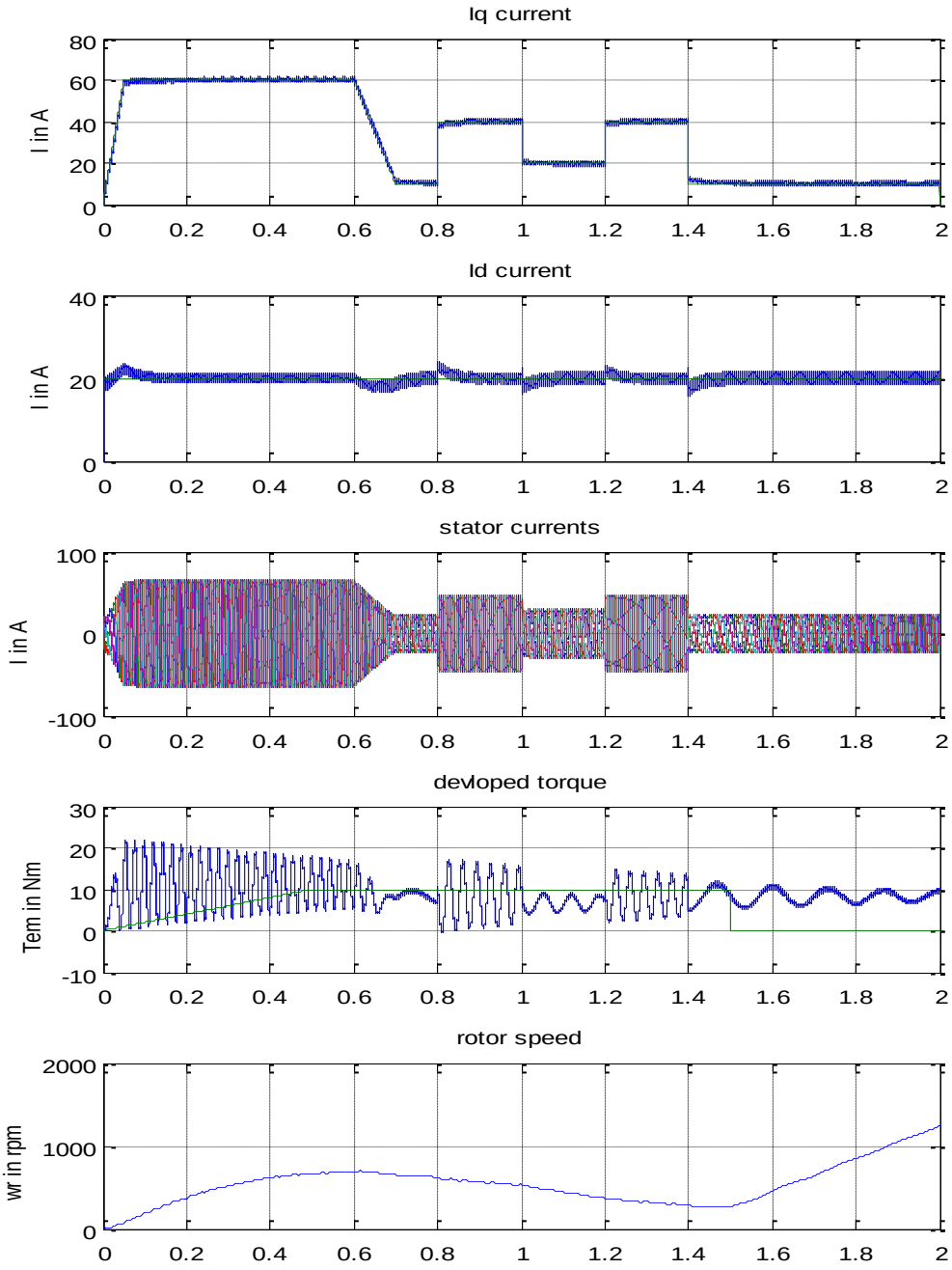

Fig. 52 : 6L Sequence (a) Iq (b) Id (c) Stator Currents (d) Torque (e) Speed

CHAPTER VII

CONCLUSIONS AND FUTURE WORK

Current research has a lot to say on shaft voltages and bearing currents. Many solutions were proposed to mitigate this problem. However, all these solution include adding cost to the system.

For five-phase induction motor, several (SVPWM) switching patterns exist. In this thesis, a new switching pattern was developed to reduce the shaft voltages and bearing currents. To implement the new scheme, only the software is modified and thus there will be no additional cost.

This new pattern is compared with conventional ones. The (6L) switching scheme was proven to reduce the shaft voltage. Depending on the system voltage levels and the breakdown voltage, this could eliminate the EDM bearing currents.

The main advantage of (6L) compared to (2L+2M) is improving the THD. Although, it keeps the dv/dt bearing current at the same level, it decreases the opportunity of EDM currents.

This work could be extended to multiphase drives with more than five-phases (e.g. seven phases) with similar switching scheme.

REFERENCES

[1] R. Hoppler and R. A. Errath, "Motor bearings, not just a piece of metal," in *IEEE-IAS/PCA Cement Industry Conference*, North Charleston, SC, 2007.

[2] J. Erdman, R. J. Kerkman, D. Schlegel and G. Skibinski, "Effect of PWM inverters on ac motor bearing currents and shaft voltage," in *Proc. IEEE-APEC Annu. Meeting*, 1995.

[3] D. Busse, J. Erdman, R. J. Kerkman, D. Schlegel and G. Skibinski, "The effects of PWM voltage source inverters on the mechanical performance of rolling bearings," in *Proc. IEEE APEC '96*, San Jose, CA, 1996, pp.

[4] D. Busse, J. Erdman, R. J. Kerkman, D. Schlegel and G. Skibinski, "An evaluation of the electrostatic shielded induction motor: a solution for rotor shaft voltage buildup and bearing current," in *Ind. Applicat.Society Conf. Rec.*, San Diego, CA, 1996.

[5] D. Busse, J. Erdman, R. J. Kerkman, D. Schlegel and G. Skibinski, "System electrical parameters and their effects on bearing currents," *IEEE Trans. Ind. Applicat.,* vol. 33, no. 2, pp. 577-584, 1997.

[6] D. Busse, J. Erdman, R. J. Kerkman, D. Schlegel and G. Skibinski, "Bearing currents and their relationship to PWM drives," *IEEE Trans. Power Electron.,* vol. 12, no. 2, pp. 243-252, 1997.

[7] S. Chen, T. Lipo and D. Fitzgerald, "Source of induction motor bearing currents

caused by PWM inverters," *IEEE Trans. Energy Convers.,* vol. 11, no. 1, pp. 25-32, 1996.

[8] S. Chen, T. Lipo and D. Fitzgerald, "Modeling of motor bearing currents in PWM inverter drives," *IEEE Trans. Ind. Appl.,* vol. 32, no. 6, pp. 1365-1370, 1996.

[9] P. Alger and H. Samson, "Shaft currents in electric machines," *A.I.R.E. Conf.,* Feb 1924.

[10] I. Onel and M. El Hachemi Benbouzid, "Induction motor bearing failure detection and diagnosis: park and concordia transform approaches comparative study," *IEEE/ASME Trans. Mechatronics,* vol. 13, no. 2, pp. 257-262, April 2008.

[11] A. Binder and A. Muetze, "Scaling effects of inverter-induced bearing currents in ac machines," *IEEE Trans. Ind. Applicat.,* vol. 44, no. 3, pp. 769 - 776, 2008.

[12] J. R. Stewart and D. D. Wilson, "High phase order transmission—a feasibility analysis, part I—steady state considerations," *IEEE Trans. Power Apparatus Syst.,* Vols. PAS-97, no. 6, p. 2300–2307, 1978.

[13] H. A. Toliyat, "Analysis and simulation of five-phase variable-speed induction motor drives under asymmetrical connections," *IEEE Trans. Power Electron.,* vol. 13, no. 4, pp. 748-756, 1998.

[14] A. Julian, T. Lipo and G. Oriti, "Elimination of common mode voltage in three phase sinusoidal power converters," in *PESC '96*, 1996.

[15] H. A. a. H. A. S. Ogasawara, "An active circuit for cancellation of common-mode voltage generated by a PWM inverter," *IEEE Trans. Power Electron,* vol. 13, no. 5,

p. 835–841, 1998.

[16] A. Hava and E. Ün, "High-performance PWM algorithm for common-mode voltage reduction in three-phase voltage source inverters," *IEEE Trans. Power Electron.*, vol. 26, no. 7, pp. 1998 - 2008, 2011.

[17] H. Toliyat, R. Shi and H. Xu, "A DSP-based vector control of five-phase synchronous reluctance motor," in *Conf. Rec. IEEE IAS Annu. Meeting*, Rome, Italy, 2000.

[18] A. Iqbal and E. Levi, "Space vector modulation schemes for a five-phase voltage source inverter," in *Proc. Eur. Conf. Power Elect. Appl.*, 2005.

[19] M. Duran and E. Levi, "Multi-dimensional approach to multi-phase space vector pulse width modulation," in *Proc. 33rd Annu. Conf. IEEE IECON*, Paris, France, 2006.

[20] H.-M. Ryu, J.-H. Kim and S.-K. Sul, "Analysis of multiphase space vector pulse width modulation based on multiple d-q spaces concept," in *IPEMC Conference*, 2004.

[21] S. Xue and X. Wen, "Simulation analysis of two novel multiphase SVPWM strategies," in *Proc. IEEE ICIT*, Hong Kong, 2005.

[22] C.-M. Ong, "Dynamic simulations of electric machinery: using MATLAB/SIMULINK, Prentice Hall PTR", 1998, pp. 433-440.

VITA

Name:	Hussain A. I. A. Hussain
Address:	c/o Dr. Hamid A. Toliyat
	Electrical Machines & Power Electronics Laboratory
	Department of Electrical Engineering
	TAMU 3128
	Texas A&M University
	College Station, Texas 77843-3128
Email Address:	hah027@tamu.edu
Education:	B.Sc., Electrical Engineering, Kuwait University, 2007